eNeuro

Research Article: New Research | Development

Neuropilin-1 and the Positions of Glomeruli in the Mouse Olfactory Bulb

Neuropilin-1 and mouse olfactory glomeruli

Bolek Zapiec, Olaf Christian Bressel, Mona Khan, Andreas Walz[†] and Peter Mombaerts

Max Planck Research Unit for Neurogenetics, 60438 Frankfurt, Germany

DOI: 10.1523/ENEURO.0123-16.2016

Received: 15 May 2016

Revised: 26 September 2016

Accepted: 30 September 2016

Published: 5 October 2016

B.Z. and O.C.B. have equal contributions. M.K. and P.M. conceived the project. B.Z., O.C.B, and M.K. performed experiments and contributed to editing the paper. A.W. generated the conditional *Nrp1* knockout strain in the laboratory at P.M. at The Rockefeller University, New York. P.M. supervised the project and wrote the paper.

Funding: Max Planck Society

Conflict of Interest: Authors report no conflict of interest.

Max Planck Society.

[†]Deceased 26 June 2013.

Correspondence should be addressed to Peter Mombaerts, Max Planck Research Unit for Neurogenetics, Max-von-Laue-Strasse 4, 60438 Frankfurt, Germany. Phone +49 69 850033 4000. Email peter.mombaerts@gen.mpg.de

Cite as: eNeuro 2016; 10.1523/ENEURO.0123-16.2016

eNeuro eN-NWR-0123-16R2 26 September 2016

1. Neuropilin-1 and the Positions of Glomeruli in the Mouse Olfactory Bulb

2. Neuropilin-1 and mouse olfactory glomeruli

3. Bolek Zapiec*, Olaf Christian Bressel*, Mona Khan, Andreas Walz†, and Peter Mombaerts. Max Planck Research Unit for Neurogenetics, 60438 Frankfurt, Germany. † Deceased 26 June 2013.

4. B.Z. and O.C.B. have equal contributions. M.K. and P.M. conceived the project. B.Z., O.C.B, and M.K. performed experiments and contributed to editing the paper. A.W. generated the conditional *Nrp1* knockout strain in the laboratory at P.M. at The Rockefeller University, New York. P.M. supervised the project and wrote the paper.

5. Peter Mombaerts, Max Planck Research Unit for Neurogenetics, Max-von-Laue-Strasse 4, 60438 Frankfurt, Germany. Phone +49 69 850033 4000. Email peter.mombaerts@gen.mpg.de

6. Number of figures: 10

7. Number of tables: 0

8. Number of multimedia: 2

9. Number of words for Abstract: 250

10. Number of words for Significance Statement: 118

11. Number of words for Introduction: 733

12. Number of words for Discussion: 2,226

13. Acknowledgements: This paper is dedicated to the memory of Andreas Walz.

14. Conflicts of interest: Authors report no conflict of interest.

15. Funding sources: Max Planck Society.

Abstract

It has been known since 1996 that mouse odorant receptors (ORs) are involved in determining the positions of the sites of coalescence of axons of olfactory sensory neurons (OSNs) - the thousands of glomeruli in the olfactory bulb. But the molecular and cellular mechanisms of OR-mediated axonal coalescence into glomeruli remain unclear. A model was proposed in 2006-2009 whereby OR-derived cAMP signals, rather than direct action of OR molecules, determine the target destinations (glomeruli) of OSNs in the bulb. This model hypothesizes that OR-derived cAMP signals determine the expression levels of neuropilin-1 (Nrp1) in OSN axon termini; that levels of Nrp1 in glomeruli form a gradient from anterior-low to posterior-high throughout the bulb; and that these Nrp1 levels mechanistically determine anterior-posterior patterning of glomeruli. Here, we describe the first independent evaluation of the Nrp1 model since it was formulated a decade ago. We test this model for the well-characterized mouse OR M71 using our gene-targeted mouse strains, which are publicly available. In contradiction to this model, we observe a variety of configurations for the M71 glomeruli in the conditional *Nrp1* knockout. We then reassess this model for the original OR transgene with which the model was developed, using the same, publicly available mouse strains. We discover that glomerular positions do not undergo the simple anterior shift that has been reported in the conditional *Nrp1* knockout for this OR transgene. Taken together, our findings

do not support the Nrp1 model for the anterior-posterior patterning of glomerular positions in the olfactory bulb.

52 **Significance statement**

53

54 In the mouse, each olfactory sensory neuron expresses one of •1,100 odorant receptor
55 genes. The odorant receptor determines to which odorants the neuron responds
56 physiologically, and in which glomerulus of the olfactory bulb its axon terminates. A
57 model was proposed 10 years ago whereby intracellular signals derived from the
58 odorant receptor determine the level of neuropilin-1, which in turn determines the
59 position of the glomerulus along the anterior-posterior axis of the bulb. We provide the
60 first test of this model, for a well-characterized odorant receptor and separately with the
61 original mouse strains that led to the formulation of the model. Our results do not
62 support the neuropilin-1 model of anterior-posterior patterning of glomerular positions
63 in the olfactory bulb.

64

Introduction

In the mouse, the 1,100 odorant receptor (OR) genes (Buck and Axel, 1991) determine to which odorants an olfactory sensory neuron (OSN) responds (Bozza et al., 2002) and in which of the 3,600 glomeruli of the olfactory bulb (Richard et al., 2010) the axon of an OSN terminates (Mombaerts, 2006). A gene-targeted replacement of the OR coding region provided the first evidence that ORs are mechanistically involved in determining the positions of glomeruli (Mombaerts et al., 1996). A set of experiments with a transgenic mouse MOR23 promoter defined by Vassalli et al., 2002 but expressing a rat OR (I7) instead of mouse MOR23, led to a model whereby OR-derived cAMP signals, rather than direct action of OR molecules, determine the target destinations (glomeruli) of OSNs (Imai et al., 2006, 2009;. Luo, 2015). This model proposes that OR-derived cAMP signals regulate the transcription of genes encoding axon guidance molecules, which then guide positioning of glomeruli along the anterior-posterior axis of the bulb. OSNs expressing rat OR I7 from a transgenic mouse MOR23 promoter form in the medial aspect of the bulb a novel, artificial glomerulus, which appears to be homogeneous in that it is not coinnervated by OSNs expressing an endogenous mouse OR (Imai et al., 2006, 2009). Immunostaining in bulb sections for the axon guidance molecule neuropilin-1 (Nrp1) in mice at postnatal day (PD) 14 revealed, in the medial aspect of the bulb, a gradient of Nrp1 expression in a row of 20 glomeruli that encompass the novel, artificial glomerulus, with low glomerular Nrp1 expression at the anterior end and high expression at the posterior end (Imai et al., 2006). By crossing a

88 conditional *Nrp1* knockout (Gu et al., 2003) with a transgene expressing rat OR I7 from a
89 mouse MOR23 promoter along with Cre recombinase, an anterior glomerular shift was
90 reported at PD14; conversely, when Nrp1 was overexpressed in these OSNs from a
91 transgene, a posterior glomerular shift was reported (Imai et al., 2009). Agonist-
92 independent G-protein coupled receptor activity was later proposed to regulate
93 anterior-posterior targeting of axons of OSNs via Nrp1 (Nakashima et al., 2013).
94 Curiously, when formulating the Nrp1 model, data were reported only for the
95 projection sites (glomeruli) in the medial aspect of the bulb (Imai et al., 2006, 2009). But it
96 is well established that glomeruli for a given OR, with a few exceptions (Strotmann et
97 al., 2000), are found both in the medial and the lateral aspects of the bulb, including the
98 MOR23 glomeruli (Vassalli et al., 2002; Zapiec and Mombaerts, 2015). Thus, it is not
99 known what impact the conditional *Nrp1* knockout has on the lateral glomerulus in
100 mice that express rat OR I7 from a transgenic mouse MOR23 promoter.
101 Here, we describe the first independent evaluation of the Nrp1 model since it was
102 formulated a decade ago. We test the model with a genetic strategy that is based on the
103 well-characterized mouse OR, M71. The M71 glomeruli reside posteriorly and are
104 Nrp1+ (Dibattista and Reisert, 2016). Our experimental design makes use of our publicly
105 available mouse strains that carry gene-targeted mutations. We avoid the use of small
106 transgenes, because these are notorious for their line-to-line variability (Vassalli et al.,
107 2002; Vassalli et al., 2011). Moreover these gene-targeted strains enable us to study
108 glomeruli that are formed by the coalescence of axons of OSNs that express a mouse OR
109 from its endogenous locus. We also create a mosaic situation whereby Nrp1+ M71+

110 OSNs coexist in the same mouse with Nrp1- M71+ axons, capitalizing on the unusual
111 modality of monoallelic OR gene expression. We observe substantial variability in the
112 configurations of M71 glomeruli in 88 bulbs examined of 47 conditional *Nrp1* knockout
113 mice, with ectopic M71 glomeruli forming anteriorly and dorsally. We then reassessed
114 the Nrp1 model by analyzing the publicly available mouse strains with which it was
115 formulated originally (Imai et al., 2009). Surprisingly, we cannot confirm the simple
116 anterior shift of the medial glomerulus that was reported in the conditional *Nrp1*
117 knockout. The lateral glomerulus undergoes typically a ventral shift, and less of an
118 anterior shift. Both medially and laterally, more than one glomerulus is present in the
119 conditional *Nrp1* knockout. The domain of the bulb that these multiple glomeruli
120 occupy can be described as a sector (medially) or belt (laterally). Taken together, our
121 results pose a challenge the Nrp1 model (Imai et al., 2006, 2009; Luo, 2015). A revision of
122 this model becomes imperative.

Materials and Methods

Generation of a gene-targeted mouse strain carrying a *Nrp1* floxed allele

We constructed a targeting vector by long-range PCR in order to generate a conditional mutation in the *Nrp1* gene by flanking exon 2 with *loxP* sites. The linearized targeting vector was electroporated in the parental embryonic stem cell line E14 of the 129P2/OlaHsd genetic background. G418-resistant clones were screened for homologous recombination by Southern blot hybridization of genomic DNA using an external probe. The FRT-flanked *neo* selectable marker was excised by Flp-mediated recombination. Our *Nrp1* floxed strain is publicly available from The Jackson Laboratory as #6707, official strain name STOCK Nrp1<tm1.1Mom>/MomJ. The design of this targeted mutation is similar to the published *Nrp1* floxed strain (Gu et al., 2003); in both strains, exon 2 of *Nrp1* is excised upon Cre recombination.

Mouse strains from other laboratories

The Cre reporter strain R26-tauGFP41, carrying the gene-targeted mutation ROSA26-CAGS-τ GFP (Mayer et al., 2010) with official allele name Gt(ROSA)26Sor<tm1(CAG-Mapt/GFP)Uboe>, was a generous gift from Uli Boehm (University of Saarland, Homburg, Germany). The gene-targeted *Nrp1* floxed strain (Gu et al., 2003) was obtained from The Jackson Laboratory as #5247, official strain name

145 B6.129(SJL)-Nrp1<tm2Ddg>/J. The transgenic strain I7-Cre-YFP Tg, also referred to as
146 I7-ires-Cre, or I7(WT)-Cre, or I7-ires-Cre-ires-gap-YFP (Imai et al., 2009), was obtained
147 from the RIKEN BRC (National Bio-Resource Project of the MEXT, Japan) as
148 #RBRC02932, official strain name C57BL/6-Tg(Olfr16-Olr226,-Cre,-EYFP)1Hsak.
149
150 **Mouse husbandry and experimentation**
151
152 Mice were maintained in specified pathogen-free conditions in individually
153 ventilated cages of the Tecniplast green line. Mice received *ad libitum* gamma-irradiated
154 ssniff V1124-727 feed (ssniff, Soest, Germany). Nesting, bedding, and enrichment were
155 provided as nestpak, Datesand Grade 6 (Datesand, Manchester, United Kingdom).
156 Mouse experiments were carried out in accordance with guidelines of the National
157 Institutes of Health and the German Animal Welfare Act, European Communities
158 Council Directive 2010/63/EU, and the institutional ethical and animal welfare
159 guidelines of the Max Planck Institute of Biophysics and the Max Planck Research Unit
160 for Neurogenetics. Approval came from the IACUC of The Rockefeller University, the
161 *Regierungspräsidium* Darmstadt, and the *Veterinäramt* of the City of Frankfurt.
162
163 **Immunohistochemistry on sections**
164
165 Mice (females and males) were anesthetized by intraperitoneal injection of
166 ketamin HCl and xylazine (210 mg/kg and 10 mg/kg body weight, respectively), and

167 perfused intracardially with ice-cold PBS followed by 4% paraformaldehyde in PBS. The
168 brain was immersed in 15% sucrose in PBS and 30% sucrose in PBS, each overnight at
169 4ºC on a shaker. After cryoprotection the brain was trimmed and frozen in O.C.T.
170 compound (Tissue-Tek) on dry ice in ethanol. Serial horizontal sections encompassing
171 the olfactory bulbs were generated with a Leica CM3050 S cryostat, set at 12 µm
172 thickness. The sections were washed with 1x PBS, and then blocked with 10 % normal
173 donkey serum, 0.3% Triton X-100 in 1x PBS for 1 hr at room temperature. After the
174 blocking step, sections were incubated in 3% BSA, 0.3% Triton X-100 in 1x PBS overnight
175 at 4˚C with primary antibodies: rabbit anti-Adcy3 (1:1000, Santa Cruz Biotechnology,
176 Dallas, TX, USA, #sc-588) and goat anti-Nrp1 (1:100, R&D systems, Minneapolis, MN,
177 USA, #AF566). Sections were then incubated at 1.5 hr at room temperature with
178 secondary antibodies: donkey anti-rabbit IgG Alexa647 (1:500, Jackson ImmunoResearch
179 Laboratories, West Grove, PA, USA, #711-606-152) for rabbit anti-Adcy3, and donkey
180 anti-goat IgG Alexa546 (1:1000, Thermo Fischer Scientific, Waltham, MA, USA,
181 #A11056) for goat anti-Nrp1. Nuclear staining was done with DAPI (1:10,000, Thermo
182 Fischer Scientific, #D1306) after the washing steps. Sections were imaged with a Zeiss
183 LSM 710 confocal microscope (Oberkochen, Germany).
184
185 **Immunolabeling of wholemounts**
186
187 Samples were processed according to the iDISCO protocol (Renier et al., 2014).
188 Primary antibodies were goat anti-Nrp1 (R&D Systems, Minneapolis, MN, USA,

#AF566), and guinea pig anti-VGLUT2 (Synaptic Systems, Göttingen, Germany, #135 404). Secondary antibodies were donkey anti-goat Alexa 488 (Thermo Fisher Scientific, #A11055), and donkey anti-guinea pig RRX (Jackson ImmunoResearch Laboratories, #706-295-148).

Serial block-face two-photon tomography

Serial block-face two-photon tomography was performed with a TissueCyte 1000 scanner (TissueVision, Cambridge, MA, USA) equipped with a Zeiss 20X 1.0NA objective and a Ti:Sapphire laser (Mai Tai HP DeepSee, Spectra-Physics, Santa Clara, CA, USA). Methods were as described in Zapiec and Mombaerts, 2015. Briefly, mechanical section thickness was set at 100 µm. Optical z-stacks were captured at an x-y resolution of 1.02 µm per pixel and 5 µm per z-plane, resulting in voxels of ~5 μm^3. Stacks were captured starting 50 µm below the cutting plane until a depth of 150 µm, thus spanning 100 µm in the z-axis. Stacks of images were processed using custom Python, Matlab, and ImageJ scripts provided by TissueVision. The 3D reconstruction and measurements were performed with Amira 6 (FEI, Hillsboro, OR, USA).

209 **Results**

210

211 **Glomeruli formed by the coalescence of axons of OSNs that express the OR gene *M71***

212

213 The subject of our first study with a conditional *Nrp1* knockout is the population
214 of OSNs that express the OR gene *M71* (M71+ OSNs), also known as *Olfr151*. The choice
215 of this OR gene is motivated by the extensive knowledge that has been collected over
216 the past 15 years, including the characterization of odorous ligands for M71 (Bozza et
217 al., 2002). We have reported 39 strains with distinct gene-targeted mutations at the *M71*
218 locus. Importantly, the strain M71-IRES-Cre (Li et al., 2004) is the only gene-targeted Cre
219 driver strain for a mouse OR gene that is publicly available.

220 M71 is expressed in a few thousand OSNs at postnatal day (PD) 21 (Bressel et al.,
221 2016). In mice that carry the gene-targeted M71-IRES-tauGFP mutation (Potter et al.,
222 2001), M71+ OSNs express tauGFP along with M71 from bicistronic transcripts. The
223 GFP+ axons typically coalesce into a single glomerulus (sometimes into two or three
224 glomeruli) posteriorly each in the medial and lateral aspects of the olfactory bulb at
225 PD21 (Fig. 1*A*). The positions of the M71 glomeruli are conserved. Crossing the M71-
226 IRES-Cre strain to the Cre reporter strain R26-tauGFP41 (Mayer et al., 2010; Wen et al.,
227 2011) phenocopies the configuration of labeled glomeruli seen in the M71-IRES-tauGFP
228 strain (Fig. 1*B*). Consistent with their posterior position in the bulb, M71 glomeruli are
229 Nrp1+ (Dibattista and Reisert, 2016).

230 Thus, the population of M71+ OSNs represents a convenient and robust model
231 system served by numerous publicly available gene-targeted strains, to assess the role of
232 Nrp1 in determining the positioning of M71 glomeruli along an anterior-posterior axis.
233
234 **Ectopic anterior and ectopic dorsal glomeruli in triple-mutant n5247MCZ mice**
235
236 We determined the effects of a conditional *Nrp1* knockout in M71+ OSNs using
237 the same *Nrp1* floxed allele (Gu et al., 2003) that was employed in Imai et al., 2009. We
238 refer to this allele as n5247, reflecting the strain number in the catalog of The Jackson
239 Laboratory, from which this strain is publicly available. By repeated crossing we
240 generated triple-mutant n5247MCZ mice. These mice are homozygous for the *Nrp1*
241 floxed allele (n5247), homozygous for the gene-targeted M71-IRES-Cre allele (MC) (Li et
242 al., 2004), and hemizygous or homozygous for the widely used Cre reporter Z/EG
243 trangene (Z) (Novak et al., 2000).
244 In triple-mutant n5247MCZ mice, M71+ OSNs express Cre and become devoid of
245 Nrp1; moreover, they become GFP+ by virtue of Cre-mediated excision of a *loxP*-
246 flanked segment of the reporter transgene that results in permanent GFP expression.
247 Examples of whole mounts of bulbs of triple-mutant n5247MCZ mice are shown for
248 postnatal day PD14 and PD21 (Fig. 1*C*,*D*): a single small GFP+ glomerulus is present
249 anteriorly, and a single large GFP+ glomerulus dorsally and posteriorly. Henceforward
250 we refer to these glomeruli as "ectopic anterior" and "ectopic dorsal". This configuration

251 deviates drastically from the typical configuration of one or a few M71 glomeruli
252 posteriorly in each of the medial and lateral aspects of the bulb (Fig. 1*A*,*B*).
253 But there is substantial variability in the configurations of sites of coalescence
254 (glomeruli) of GFP+ axons, when we examined a total of 45 bulbs of 23 triple-mutant
255 n5247MCZ mice at 5 ages (Fig. 2*A*): 10 bulbs at PD0 (when the glomeruli are beginning
256 to form), 8 at PD14, 21 at PD21, 2 at PD45, and 4 at PD105. In attempt to discern distinct
257 categories, we identified at least four configurations of GFP+ glomeruli, which we refer
258 to as I, II, III, IV. Configuration I (22/45 bulbs, 49%) is the most common: it consists of a
259 single small ectopic anterior glomerulus and a single large ectopic dorsal glomerulus,
260 and is exemplified in the bulbs shown in Fig. 1*C*,*D*. Configuration II (16 bulbs, 36%)
261 comprises a single small ectopic anterior glomerulus and two glomeruli posteriorly.
262 Configuration III consists of a single large ectopic dorsal glomerulus but no ectopic
263 anterior glomerulus (4 bulbs, 9%). Configuration IV has two dorsal glomeruli
264 posteriorly but no ectopic anterior glomerulus (3 bulbs, 7%). Bulbs with an ectopic
265 anterior glomerulus (or a developing ectopic anterior glomerulus, at PD0) thus occur in
266 84% of bulbs (I+II, 38/45), and bulbs with a single large ectopic dorsal glomerulus in
267 58% of bulbs (I+III, 26/45). An ectopic anterior glomerulus is present in 80% of bulbs
268 (8/10) at PD0. At PD105, the oldest age examined, there are no ectopic anterior
269 glomeruli in any bulb (4/4). For comparison with Imai et al., 2009, which report data
270 about PD14 mice, the configuration that we observe most frequently at PD14 is II (6/8,
271 75%): a single small ectopic anterior glomerulus and two posterior glomeruli.

We have described a linear relationship between the number of OSNs that express a given OR gene and the total volume of the corresponding glomeruli in the bulbs (Bressel et al., 2016). We find that in n5247MCZ mice at PD22, the ectopic anterior glomeruli contribute 20.0% (STDEV ± 6.5%) to the total glomerular volume per mouse, using methods outlined in Bressel et al., 2016. It follows that ~20% of Nrp1- M71+ OSNs innervate these EA glomeruli.

Thus, the multiple configurations of M71 glomeruli in a conditional *Nrp1* knockout and the substantial variability are not consistent with the Nrp1 model for anterior-posterior patterning of glomeruli (Imai et al., 2006, 2009). This model, which was formulated based on results from mice expressing a rat OR from a transgenic mouse MOR23 promoter, does not apply to the first tested population of OSNs that express a mouse OR from its endogenous locus, *M71*.

Three-dimensional reconstructions of the bulbs of triple-mutant n5247MCZ mice

The variability in configurations of M71 glomeruli in the conditional *Nrp1* knockout poses an unexpected experimental challenge. There are variations on a theme, and further examination may reveal additional configurations or subconfigurations. To enable a direct comparison of the positions of M71 glomeruli with and without Nrp1, we imaged bulbs using TissueCyte serial block-face two-photon tomography (Ragan et al., 2012), and generated three-dimensional (3D) reconstructions of bulbs (Zapiec and

294 Mombaerts, 2015). We made use of the intrinsic fluorescence signal in glomeruli in four
295 bulbs of PD21 mice homozygous for the gene-targeted M71-IRES-tauYFP mutation
296 (Nrp1+) and in six bulbs of triple-mutant n5247MCZ mice (Nrp1-) also at PD21.
297 Methods of image acquisition, registration, and image processing have been described
298 in detail (Zapiec and Mombaerts, 2015). Figure 3 and Movie 1 show views of the merged
299 right olfactory bulb, which is composed of a total of 10 left or right olfactory bulbs. The
300 views on this merged bulb are, respectively, dorsal and comparable to Figure 1 (Fig. 3*A*),
301 and dorsomedial and slightly tilted laterally (Fig. 3*B*) so that the posterior-medial
302 glomeruli are better visible. Figure 3*C* provides close-ups. All four M71-IRES-tauYFP
303 bulbs have a single medial glomerulus posteriorly; two have a single lateral glomerulus
304 posteriorly, and two have two lateral glomeruli posteriorly. These configurations are
305 consistent with what has been reported for M71 glomeruli in several gene-targeted
306 strains at or around PD21 (for instance, Potter et al., 2001; Feinstein and Mombaerts,
307 2004; Feinstein et al., 2004; Zou et al., 2004). The configuration of glomeruli in the 3D
308 reconstructions of bulbs of triple-mutant n5247MCZ mice deviates drastically from that
309 in the M71-IRES-tauYFP mice. Four n5247MCZ bulbs show configuration I (Fig. 2*A*),
310 with a single EA glomerulus and a single ectopic dorsal glomerulus; this configuration
311 is the most frequently seen at PD21. One n5247MCZ bulb is of configuration II (one
312 ectopic anterior glomerulus and two glomeruli posteriorly), and another n5247MCZ
313 bulb of configuration III, with a single ectopic dorsal glomerulus. New information from
314 these 3D reconstructions is that the ectopic dorsal glomeruli reside roughly halfway

315 between the medial and lateral M71 glomeruli, and at approximately the same anterior-
316 posterior position.
317 Thus, the 3D reconstructions of bulbs by serial block-face two-photon
318 tomography confirm and extend the observations made by wholemount
319 epifluorescence. The multiple configurations of M71 glomeruli and the substantial
320 variability are not consistent with the Nrp1 model for anterior-posterior patterning of
321 glomeruli.
322
323 **Quadruple-mutant NMRCZ mice**
324
325 OR genes are expressed monoallelically: an OSN that expresses a given OR gene
326 expresses one allele of it (Chess et al., 1994; Strotmann et al., 2000; Ishii et al., 2001). This
327 monoallelic expression is extremely tight (Saraiva et al., 2015). Next, we developed a
328 novel genetic strategy that capitalizes on this unusual modality of gene expression in the
329 mouse. The quadruple-mutant mice NMRCZ enable a direct, mosaic comparison of
330 Nrp1+ and Nrp1- populations of M71+ OSNs within the same mouse, as follows.
331 We generated a novel floxed allele of *Nrp1* by flanking exon 2 with *loxP* sites,
332 adopting a similar design as for the published *Nrp1* floxed allele (Gu et al., 2003). We
333 then produced two triple-mutant strains by repeated crossing: NMCZ and NMRZ. The
334 triple-mutant strain NMCZ is homozygous for our *Nrp1* floxed allele (N), homozygous
335 for M71-IRES-Cre (MC), and hemizygous or homozygous for the Z/EG transgene (Z); it
336 is analogous to the triple-mutant n5247MCZ strain but with our *Nrp1* floxed allele. As in

337 triple-mutant n5247MCZ mice, ectopic glomeruli exist also in triple-mutant NMCZ
338 mice, both the large ectopic dorsal glomerulus (Fig. 4*A*) and the smaller ectopic anterior
339 glomerulus (Fig. 4*B*). The triple-mutant strain NMRZ is homozygous for our *Nrp1*
340 floxed allele (N), homozygous for M71-IRES-tauRFP2 (Li et al., 2004) (MR), and
341 hemizygous or homozygous for the Z/EG transgene (Z). By crossing an NMCZ mouse
342 with an NMRZ mouse, quadruple-mutant NMRCZ offspring are obtained that are
343 homozygous for our *Nrp1* floxed allele (N), compound heterozygous at the *M71* locus
344 (M71-IRES-Cre and M71-IRES-tauRFP2) (MRC), and hemizygous or homozygous for the
345 Z/EG reporter (Z). In these quadruple-mutant mice, OSNs that express the M71-IRES-
346 tauRFP2 allele are RFP+ and Nrp1+, and OSNs that express the M71-IRES-Cre allele are
347 GFP+ via expression of the Z/EG reporter, and Nrp1-.

348 We analyzed a total of 43 bulbs of 24 quadruple-mutant NMRCZ mice at 6 ages: 3
349 at PD7, 8 at PD14, 13 at PD21, 11 at PD35, 4 at PD45, and 4 at PD70 (Fig. 2*B*). There are
350 no bulbs of configuration II, which we had identified earlier in triple-mutant n5247MCZ
351 mice. In addition to the configurations I (4 bulbs, 9%), III (2 bulbs, 5%), and IV (9 bulbs,
352 21%), we identify two new configurations in quadruple-mutant NMRCZ mice. In
353 configuration V (Fig. 4*C* right and 4*D*), the most frequent configuration (26 bulbs, 60%),
354 there is a single small ectopic anterior glomerulus anteriorly (Fig. 4*E*,*J*), a single medial
355 glomerulus (Fig. 4*G*), and a single large ectopic dorsal glomerulus (Fig. 4*H*). The medial
356 glomerulus is innervated clearly in a mixed fashion, but to various extents, by RFP+
357 axons and by GFP+ axons. The position of this medial glomerulus is typical for the
358 medial M71 glomerulus. Configuration VI (2 bulbs, 4%) has the same glomeruli as

359 configuration V plus a single lateral glomerulus, at a position that is typical for the
360 lateral M71 glomerulus (Fig. 4*C* left and 4*F*). Taken together, in 65% of bulbs (V+VI,
361 28/43), the RFP+ axons (representing the M71-IRES-tauRFP2 allele, without Cre
362 recombination) coalesce into glomeruli at positions that are typical for M71 glomeruli,
363 and they mix in these glomeruli with GFP+ axons (representing the M71-IRES-Cre allele,
364 with Cre recombination) (Fig. 4*I*).
365 The numbers of labeled OSNs in the triple-mutant and quadruple-mutant mice
366 are comparable to those in M71-IRES-tauGFP and M71-IRES-tauRFP2 mice at PD21 (Fig.
367 5): n5247MCZ t-test p=0.70, NMRCZ t-test p=0.34. These numbers were determined
368 with Abercrombie correction, as detailed in Bressel et al., 2016. We do not find a
369 significant difference between the numbers of labeled OSNs expressing the M71-IRES-
370 Cre or M71-IRES-tauRFP2 allele in NMRCZ mice (t-test p=0.85).
371
372 **Glomeruli in posterior domains of the bulb can be Nrp1+ or Nrp1-**
373
374 Nrp1 expression in OSNs is dependent on expression of the cAMP-generating
375 enzyme adenylate cyclase Adcy3 (Dal Col et al., 2007). Most if not all mature OSNs
376 express Adcy3. An exception is a population of chemosensory neurons in the mouse
377 main olfactory epithelium that express the cation channel Trpc2 (Liman et al., 1999), the
378 cyclic-nucleotide gated channel subunit Cnga2, and the guanylate cyclase Gucy1b2: they
379 do not express Adcy3 (Omura and Mombaerts, 2014; 2015). Glomeruli of Gucy1b2+
380 neurons can be examined easily and specifically in mice of the gene-targeted Gucy1b2-

381 IRES-tauGFP strain: neurons that express Gucy1b2 coexpress GFP, and the expression
382 level is high enough to visualize the signal in glomeruli by the intrinsic fluorescence of
383 GFP (Omura and Mombaerts, 2015). Axons of Gucy1b2+ neurons coalesce typically into
384 three glomeruli posteriorly in the olfactory bulb (Omura and Mombaerts, 2015). The
385 absence of Adcy3 expression in Gucy1b2+ neurons and the morphological similarity
386 between Gucy1b2+ glomeruli and canonical glomeruli formed by the coalescence of
387 axons of OR-expressing OSNs predict that Gucy1b2 glomeruli are Nrp1-.
388 On a horizontal section at an extremely ventral level through the bulb of a
389 homozygous Gucy1b2-IRES-tauGFP mouse at 4 weeks, a single GFP+ glomerulus can be
390 observed at a lateral position (Fig. 6*A*). This glomerulus is Adcy3- and Nrp1-.
391 Interestingly, numerous glomeruli anterior to this GFP+ glomerulus are Adcy3+ but
392 Nrp1-, thus breaking the causal link between Adcy3 and Nrp1 expression. On a
393 horizontal section at a slightly more dorsal level, another GFP+ glomerulus at a medial
394 position is also Adcy3- and Nrp1-, and adjacent glomeruli are Adcy3+ but are either
395 Nrp1+ or Nrp1- (Fig. 6*B*). At an intermediate dorsal-ventral level of this bulb, a third
396 GFP+ glomerulus, at a lateral position, is Adcy3- and Nrp1- but the glomeruli just
397 anterior to it are Adcy3+ and Nrp1- or very weakly Nrp1+ (Fig. 6*C*).
398 Thus, by examining three posterior domains of a bulb that are defined by
399 Gucy1b2+ glomeruli, we find that there is no absolute link between Adcy3 and Nrp1
400 expression, and that posterior glomeruli can be either Nrp1+ or Nrp1-.
401

402 **Nrp1 levels in a three-dimensional reconstruction of a bulb of a wild-type C57BL6/J**
403 **mouse**
404
405 It thus became necessary to take a bulb-wide view of Nrp1 levels, and to revisit
406 the proposed anterior-posterior Nrp1 gradient (Imai et al., 2006, 2009), at the level of the
407 entire bulb and in 3D (Zapiec and Mombaerts, 2015).
408 We performed whole-mount Nrp1 immunofluorescence of wild-type C57BL/6J
409 bulbs at PD14 using the iDISCO protocol (Renier et al., 2004), and imaged and
410 reconstructed the labeled bulbs by applying serial block-face two-photon tomography.
411 Figure 7 shows a representative bulb. The Nrp1 antibody labels glomeruli efficiently,
412 but it also labels OSN axons in the olfactory nerve layer (Fig. 7*A*), thus obscuring the
413 glomeruli in 3D reconstructions of the bulb. Although we could assess the Nrp1 levels
414 within individual glomeruli when examining the tomography sections, we wanted to
415 obtain a global view of the 3D reconstructed bulb, requiring segmenting the glomerular
416 layer from the olfactory nerve layer. This segmenting was accomplished by colabeling
417 with an antibody for VGLUT2, a robust marker of glomeruli that labels OSN axon
418 terminals within glomeruli (Richard et al., 2010). We used the VGLUT2 signal to define
419 the glomeruli by thresholding this signal to perform semi-automated segmentation. By
420 masking the Nrp1 signal to display only the voxels that belong to glomeruli as defined
421 by the VGLUT2 signal (Fig. 7*B*), we visualized the intensity of the Nrp1
422 immunofluorescence signal specifically in glomeruli, and hereby obtained clear views of
423 Nrp1 levels in glomeruli across the 3D reconstructed bulb.

424 A medial view (Fig. 7*C*) and a lateral view (Fig. 7*D*) of the 3D reconstruction
425 reveal that, generally, Nrp1-low glomeruli reside anteriorly and dorsally, and Nrp1-
426 high glomeruli posteriorly. But upon closer examination, the pattern of Nrp1 levels is
427 mosaic and patchy: there is considerable variability in staining intensity among
428 neighboring glomeruli. Nrp1-low glomeruli can be found in the immediate vicinity of
429 Nrp1-high glomeruli, as we had observed in the three posterior domains defined by
430 Gucy1b2+ glomeruli. The olfactory bulb is often described as comprising two mirror-
431 image maps of glomeruli (two half-bulbs) (Nagao et al., 2000) such that glomeruli for a
432 given OR can be found in positions reflected along a mirror plane. But no such
433 symmetry is obvious when we examined the patterns of Nrp1 immunofluorescence
434 signal intensities among the medial and lateral aspects of the bulb.
435 Further quantitative analyses will be required to settle definitively the hypothesis
436 of a smooth anterior-posterior bulb-wide Nrp1 gradient, and across various possible
437 anterior-posterior "axes". Several pre- and postnatal ages must also be examined.
438
439 **Glomeruli formed by the coalescence of axons of OSNs that express the rat OR I7**
440 **from a transgenic mouse MOR23 promoter with and without Nrp1**
441
442 We felt compelled to seek to replicate the experiments with the transgenic mice
443 that express the rat OR I7 from a mouse MOR23 promoter along with the Cre
444 recombinase and gap-YFP (Imai et al., 2009). This mouse strain is publicly available
445 from the RIKEN BioResource Center, and is here referred to as I7-Cre-YFP Tg. In the

446 gap-YFP marker, the 20 N-terminal amino acid residues of GAP43 are fused to the N
447 terminus of the yellow fluorescent protein (YFP) to target it to the plasma membrane
448 (Moriyoshi et al., 1996). Figure 8*A* shows epifluorescence wholemount images of the
449 medial and lateral aspects of a left and a right bulb of two I7-Cre-YFP Tg mice at PD17,
450 visualizing the intrinsic fluorescence from the gap-YFP fusion protein. We confirm and
451 extend the observation (Imai et al., 2009) that axons expressing rat OR I7 from this
452 transgenic mouse MOR23 promoter coalesce into a single glomerulus in the medial
453 aspect of the bulb, and add that a single labeled glomerulus is present in the lateral
454 aspect of the bulb.

455 We then crossed I7-Cre-YFP-Tg mice to gene-targeted mice carrying the *Nrp1*
456 floxed allele n5247 (Gu et al., 2003), thus reproducing the same cross used in Figure 1A
457 of Imai et al., 2009. Figure 8*B* shows epifluorescence wholemount images of the medial
458 and lateral aspects of six bulbs of six I7-Cre-YFP Tg littermates at PD14, the same age
459 analyzed in Imai et al., 2009. We make distinct observations for the medial and lateral
460 aspects of these bulbs. Medially, we observe two labeled glomeruli in five of the six
461 bulbs, and four labeled glomeruli in one bulb. One of these glomeruli appears larger
462 than the others, and is more anterior except in the case of the four labeled glomeruli, of
463 which the largest is the second most anterior glomerulus. A virtual line drawn between
464 the labeled glomeruli in a given bulb yields various orientations or axes, which are
465 grossly along the anterior-posterior dimension but also have a ventral or dorsal
466 component. Laterally, we observe two to six labeled glomeruli (average 3.5), with one
467 glomerulus larger than the others. Connecting the labeled glomeruli in a given bulb

468 does not reveal a consistent orientation or axis. Because there is no information about
469 the labeled glomeruli in the lateral aspect of the bulb in Imai et al., 2009, a comparison of
470 the data is not possible.

471 Thus, the positions of the labeled glomeruli and their substantial variability in the
472 I7-Cre-YFP Tg x n5247-flox cross are not consistent with the Nrp1 model for anterior-
473 posterior patterning of glomeruli for this novel, artificial population of OSNs that
474 express rat OR I7 from a transgenic mouse MOR23 promoter.

475

476 **Three-dimensional reconstructions of the bulbs of I7-Cre-YFP Tg mice with and**
477 **without Nrp1**

478

479 Lastly, as we had done for triple-mutant n5247MCZ mice, we imaged labeled
480 bulbs of I7-Cre-YFP Tg mice with and without Nrp1, by applying serial block-face two-
481 photon tomography based on the intrinsic fluorescence of the gap-YFP marker and then
482 generating 3D reconstructions of the bulbs.

483 Figure 9 shows one example of a reconstructed (right) bulb of a I7-Cre-YFP Tg
484 mouse at PD14; it is the same bulb as shown in the bottom right panels of Fig. 8*B*. For
485 comparison the epifluorescence wholemount images of the same bulb are shown again.
486 The two labeled glomeruli in the medial aspect that were seen in the epifluorescence
487 wholemount image are clearly detectable in the 3D reconstruction. In the lateral aspect,
488 a fifth, small labeled glomerulus is detectable in the 3D reconstruction, but not seen in
489 the epifluorescence wholemount image.

Figure 10*A* shows a merged bulb of three I7-Cre-YFP Tg bulbs at PD14 including the bulb shown in Figure 9. The 3D reconstruction reveals a single labeled glomerulus in each the medial and lateral aspects of the bulb. The advantage of the merged bulb approach is that glomerular positions can be compared directly: we find that the three glomeruli are tightly clustered in each the medial and lateral aspects. In sharp contrast, the merged bulb composed of eight I7-Cre-YFP Tg x n5247-flox bulbs and the three I7-Cre-YFP Tg bulbs at PD14 (thus 11 bulbs in total) reveals a broad scattering of multiple I7-Cre-YFP Tg x n5247-flox glomeruli both in the medial and lateral aspects of the bulb (Fig. 10*B*). Medially, the scattered glomeruli (mean 2.3, minimum 1, maximum 5) occupy a broad domain of the bulb that can best be characterized as a sector, anchored at the position of the tightly clustered glomeruli of the I7-Cre-YFP Tg bulbs and radiating anteriorly and ventrally. Laterally, the scattered glomeruli (mean 3.0, minimum 2, maximum 5) are centered at the tightly clustered glomeruli of the I7-Cre-YFP Tg bulbs; 7 glomeruli underwent a dorsal shift, 14 a ventral shift, and 3 no shift. A ventral view of this merged bulb (Fig. 10*B*) reveals that the glomeruli occupy a belt that spans the ventral extent and connects the medial and lateral domains of the I7-Cre-Tg glomeruli with Nrp1. This glomerular belt is interrupted for a segment defined by the ventral ridge of the bulb. In three I7-Cre-YFP Tg x n5247-flox bulbs at PD21, there are more labeled glomeruli (medially: mean 6, minimum 4, maximum 9; laterally: mean 5.7, minimum 3, maximum 8), and the degree of scattering both medially and laterally is increased (Fig. 10*C*). The distribution of glomeruli in the PD14 and PD21 bulbs can be evaluated in Movie 2.

512 Taken together, our observations with the cross I7-Cre-YFP Tg x n5247-flox at the
513 same age of PD14 are not consistent with the data reported in Imai et al., 2009. Our
514 findings do not support the Nrp1 model of anterior-posterior patterning of glomeruli in
515 the bulb for this novel population of OSNs that express rat OR I7 from a transgenic
516 mouse MOR23 promoter.
517
518
519

Discussion

Naturally, any model that aspires to explain how axons of ~1,100 populations of OSNs each expressing a distinct OR gene sort and coalesce into ~3,600 glomeruli at conserved positions in the olfactory bulb, needs to be tested for more than a single OR gene. The Nrp1 model (Imai et al., 2006, 2009; Luo, 2015) was developed for one OR (rat OR I7), which was either FLAG-or HA-epitope tagged, expressed from a small transgenic mouse MOR23 promoter, and glomeruli were examined solely for the medial aspect of the bulb. In the intervening decade, the Nrp1 model has not been extended to an endogenous mouse OR, or to any other OR. We have here sought to assess the validity of the Nrp1 model for another population of OSNs, which express mouse OR M71 from the endogenous *M71* locus, using our publicly available, gene-targeted mouse strains. The configurations of M71 glomeruli that we discern in the conditional *Nrp1* knockouts with two distinct *Nrp1* floxed alleles are not consistent with this Nrp1 model. Moreover we cannot confirm the simple anterior shift in medial projection sites for the population of OSNs expressing rat OR I7 from a transgenic mouse MOR23 promoter; the lateral projection sites, which were not examined (Imai et al., 2006, 2009), typically undergo a ventral shift, and less of an anterior shift.

The Nrp1 model for anterior-posterior positioning of glomeruli does not apply to the native population of OSNs expressing mouse OR M71 from the endogenous *M71* locus

542

543 We observe multiple configurations and substantial variability in the patterns of
544 labeled glomeruli when Nrp1 is knocked out conditionally in M71+ OSNs. Further
545 examination may reveal additional configurations or subconfigurations.
546 We discern four configurations in triple-mutant n5247MRZ mice, in which all
547 M71+ OSNs are Nrp1-. In quadruple-mutant NMRCZ mice, in which half of M71+
548 OSNs are Nrp1+ and the other half lack are Nrp1-, we discern five configurations, of
549 which three are shared with n5247MRZ mice. A common observation is the occurrence
550 of novel, ectopic glomeruli, anteriorly and/or dorsally. The ectopic anterior glomeruli
551 are formed by ~20% of Nrp1- M71+ OSNs. Their far-anterior ectopic location is
552 strikingly reminiscent of the ectopic anterior glomeruli reported by two groups in
553 constitutive Adcy3 knockout mice, for M71 (Zou et al., 2007) and for M72 (Dal Col et al.,
554 2007), an OR that is highly related to M71. The lack of Nrp1 expression in Adcy3
555 knockout mice (Dal Col et al., 2007) suggests a possible mechanistic link between OR
556 expression, cAMP generation through Adcy3, and Nrp1 expression.
557 Our experiments on M71 with two *Nrp1* floxed alleles including the one used by
558 Imai et al., 2009, are not consistent with the model, in that we do not observe a simple
559 anterior shift of M71 glomeruli when Nrp1 is knocked out conditionally in M71+ OSNs.
560 The single large ectopic dorsal glomerulus that we observe frequently is not shifted
561 along an anterior-posterior axis at all, but resides halfway the medial and lateral M71
562 glomeruli.
563

The Nrp1 model for anterior-posterior positioning of glomeruli does not apply to the novel population of OSNs expressing rat OR I7 from a transgenic mouse MOR23 promoter

During the course of this project, we realized that we needed to take a step back and seek to reproduce the core original findings with which the Nrp1 model was formulated (Imai et al., 2009). With publicly available strains we generated the same cross of Cre driver strain and *Nrp1* floxed allele, but our observations differ. Instead of a single projection site (glomerulus) shifting anteriorly at PD14, we observe multiple glomeruli formed by the coalescence of axons expressing rat OR I7 from a transgenic mouse MOR23 promoter. When viewed in a merged bulb after 3D construction, together these medial glomeruli occupy a broad domain of the bulb that can best be characterized as a sector that is anchored posteriorly on the tightly clustered medial glomeruli in the transgenic mice with Nrp1. This sector radiates anteriorly and ventrally along various vectors, and is not consistent with a simple shift along an anterior-posterior "axis" of the bulb; at best, the vectors have an anterior component. This sector may reflect the domain of the bulb within which these axons, now devoid of Nrp1, are allowed to navigate. We then proceeded to flip these bulbs and examined the labeled glomeruli in the lateral aspect, which were not documented in Imai et al., 2006, 2009. We discovered that the scattering of the glomeruli is even more pronounced in the lateral than in the medial aspect. Together these lateral glomeruli occupy a domain of the bulb that can be regarded as a belt or a band, centered at the tightly clustered lateral

586 glomeruli in the mice with Nrp1 and extending toward the medial aspect along the
587 ventral ridge. Seven out of 24 lateral glomeruli are shifted dorsally compared to the
588 lateral glomeruli in the mice with Nrp1, but most (14/24) are shifted ventrally; the
589 remaining 3 glomeruli showed no shift. No glomeruli underwent a simple shift along an
590 anterior-posterior "axis" of the bulb.

591 At PD21 the scattering of glomeruli appears to have increased, with glomeruli
592 radiating further within the sector (medially) and the belt (laterally). We have not
593 examined mice at older ages. There may thus be a phenomenon of dynamic instability
594 when mechanisms of axonal coalescence of OSNs are perturbed by a conditional *Nrp1*
595 knockout in one particular population of OSNs. In this context, it must be kept in mind
596 that the glomeruli that are formed by the coalescence of axons expressing rat OR I7 from
597 a transgenic mouse MOR23 promoter are novel and artificial: they do not exist in wild-
598 type, non-transgenic mice.

599 Possible explanations for the discrepancy in our findings with Imai et al., 2006,
600 2009, as far as the medial aspect of the bulb is concerned are a higher quality of our
601 epifluorescence wholemount imaging, and the new method of 3D reconstruction with
602 serial block-face two-photon tomography (Zapiec and Mombaerts, 2016). Unfortunately,
603 the lateral aspect of the bulb was not examined in Imai et al., 2006, 2009.

604

605 **Asssessment of Nrp1 gradients in the bulb**

606

It is intrinsically difficult to provide convincing evidence of a Nrp1 protein gradient across the bulb, extending smoothly from anterior-low to posterior-high, at various dorsal-ventral levels, both in the medial and lateral aspects of the bulb, and at relevant ages. We have here tested the concept of a Nrp1 gradient in two ways, and with the same Nrp1 antibody as used in Imai et al., 2006, 2009. By conventional immunofluorescence we examined three posterior domains at several dorsal-ventral levels in the vicinity of Gucy1b2+ glomeruli, which are Adcy3- and Nrp1-. We find that there are Nrp1+ and Nrp1- glomeruli in these posterior domains, thus breaking the link between Adcy3 and Nrp1 expression, and constituting numerous exceptions to the notion that posterior glomeruli are Nrp1+. Moreover there is substantial heterogeneity within these posterior domains: some glomeruli adjacent to Gucy1b2+ glomeruli are Nrp1+ (and Adcy3+) and others are Nrp1- (but also Adcy3+). Serial block-face two-photon tomography (Zapiec and Mombaerts, 2015) is an advanced imaging method, enabling us to quantify Nrp1 immunofluorescence levels in each of the thousands of glomeruli of the bulb. With this method we were unable to identify consistent, robust, smooth gradients of Nrp1 across glomeruli along any axis, including possible anterior-posterior axes; but the absence of evidence for a bulb-wide gradient in our hands is not evidence for its absence. Our 3D reconstructions reiterate the difficulty in the unambiguous definition of any "axis" in the olfactory bulb (Zapiec and Mombaerts, 2015): there are no landmarks, no fiduciary points to determine "anterior" and "posterior" accurately and reproducibly and to the level of precision that is required to assess gradients rigorously and critically. Nonetheless we find that, generally, anterior

629 glomeruli are Nrp1-low and, generally, the posterior bulb has glomeruli that are Nrp1-
630 high. But Nrp1 levels do not form a simple gradient from anterior-low to posterior-high
631 throughout the bulb. Instead the Nrp1 pattern is complex and can better be described as
632 mosaic or patchy, or even idiosyncratic, with the posterior bulb hosting glomeruli that
633 are strongly Nrp1+ but intermingled with Nrp1-low glomeruli.
634
635 **Glomerular Nrp1 levels in the literature**
636
637 Our observations of mosaic, patchy patterns of Nrp1 levels across glomeruli in
638 sections and in the 3D reconstructed bulbs are consistent with the literature. An early
639 study in rat reported that "Neuropilin-1 immunoreactivity was confined to the
640 rostrolateral and caudal glomeruli of the main olfactory bulb. Moderate neuropilin-1
641 immunoreactivity was observed in most glomeruli, whereas a small number of
642 glomeruli was either very strongly labeled or unlabeled" (Pasterkamp et al., 1998).
643 Another group reported in adult mice that "NP1$^+$ olfactory axons projected selectively to
644 glomeruli within two compartments, the lateral band and the medial band. NP1$^+$
645 glomeruli (which receive NP1$^+$ olfactory axons) were completely excluded from the
646 anteromedial region and the ventral region" (Taniguchi et al., 2003). A third group
647 observed in PD5 mice that "Npn-1$^+$ glomeruli in the rostral-most 600 μm of the olfactory
648 bulb were variable in size and intensity of staining..." and "At no position along the
649 entire rostrocaudal axis of the olfactory bulb were there detectable glomeruli containing
650 npn-1$^+$ axons near the ventral midline of the olfactory bulb of wild-type mice"

651 (Schwarting et al., 2004). The Nrp1 patterns in mice were studied in detail in an attempt
652 to explain the phenotype of mice with a knockout of Sema3A, a ligand for Nrp1
653 (Schwarting et al., 2000; 2004; Taniguchi et al., 2003): Sema3A at the ventral midline
654 would guide Nrp1+ axons to regions in the lateral and medial bulb. Dibattista and
655 Reisert, 2016 wrote "... we observed a mosaic pattern of Nrp1 expression in sagittal
656 section of the olfactory bulb. Glomeruli showed high, low, or even absent levels of
657 Nrp1..." Thus, at least four groups have reported on Nrp1 levels in glomeruli of rat and
658 mouse since 1998, and like we, none have identified a gradient or gradient-like pattern
659 of Nrp1 levels throughout the bulb.
660
661 **What then may Nrp1 do in axonal wiring of OSNs?**
662
663 Puzzlingly, there are no clear commonalities in the phenotypes of the conditional
664 *Nrp1* knockout between the two populations of OSNs that we studied, although both
665 populations reside in the dorsal MOE and project their axons to glomeruli in the dorsal
666 bulb. When a Cre driver strain for another OR gene becomes available, it is possible that
667 yet another spectrum of phenotypes will be observed. Regardless how strong the effects
668 of the conditional *Nrp1* knockouts are on the number and positions of glomeruli, our
669 observations for these two populations of OSNs cannot be interpreted in terms of Nrp1
670 levels determining glomerular positions along the anterior-posterior axis. Our findings
671 leave unanswered the broader question as to whether and how OR-specific cAMP
672 signals direct axonal targeting in the olfactory system.

673 A similar variability for the same *Nrp1* floxed allele (Gu et al., 2003) was reported
674 for axons of chemosensory neurons from the Grueneberg ganglion (a specialized
675 olfactory subsystem) that express *Gucy2g* (Matsuo et al., 2012). One explanation is that in
676 the absence of Nrp1, OSN axons are free to enter into or navigate across otherwise
677 restricted regions of the bulb (such as regions where Sema3A is present), resulting in
678 multiple options for sites where Nrp1- axons can coalesce into glomeruli. We speculate
679 that for OSNs expressing rat OR I7 from a transgenic mouse MOR23 promoter,
680 the "belt" represents the degree of freedom in the lateral aspect of the bulb that a
681 conditional *Nrp1* knockout affords to axons of OSNs expressing rat OR I7 from a
682 transgenic mouse MOR23 promoter. In the absence of Nrp1, the positional variability of
683 glomeruli that is observed normally (Zapiec and Mombaerts, 2005) is greatly increased,
684 but without a clear set of rules between medial and lateral aspects, and between the two
685 populations of OSNs that we studied. In any case, Nrp1 contributes to reducing the
686 complexity of the challenging task for axons of OSNs expressing a given OR to coalesce
687 into one or a few glomeruli in highly restricted domains on the bulb.
688
689 **Conclusion**
690
691 Taken together, our results with gene-targeted mice expressing mouse OR M71
692 from the endogenous *M71* locus and transgenic mice expressing rat OR I7 from a mouse
693 *MOR23* promoter pose a challenge to the Nrp1 model that was formulated by Imai et al.,
694 2006, 2009 and that has made it into a textbook (Luo, 2015). A revision, reformulation, or

695 refinement of this model becomes thus imperative. The lack of public availability of Cre
696 driver strains for other OR genes, in particular of gene-targeted strains, precludes
697 additional experiments with conditional *Nrp1* knockouts. Our analyses of Nrp1 levels in
698 3D reconstructed bulbs and a survey of the literature do not provide evidence for
699 smooth, continuous, or fine-grained gradients of Nrp1 along any axis of the bulb,
700 including along anterior-posterior axes. Moreover, it remains difficult to define and to
701 measure "the" anterior-posterior axis of the bulb in a meaningful and comparable
702 manner. We deem it unlikely that Nrp1 determines positioning in a simple,
703 straightforward, and uniform fashion along "the" or an anterior-posterior axis for the
704 3,600 glomeruli of the mouse olfactory bulb. Nonetheless we hope that our intriguing
705 observations of a sector and belt of scattered glomeruli in I7-Cre-YPF Tg x n5247-flox
706 mice may provide clues about the mechanisms whereby a conditional *Nrp1* knockout
707 exerts such strong effects on the axonal coalescence of OSNs that express the same OR.

708 **References**
709

710 Bozza T, Feinstein P, Zheng C, Mombaerts P (2002) Odorant receptor expression defines
711 functional units in the mouse olfactory system. J Neurosci 22:3033-3043.
712

713 Bressel OC, Khan M, Mombaerts P (2016) Linear correlation between the number of
714 olfactory sensory neurons expressing a given mouse odorant receptor gene and the total
715 volume of the corresponding glomeruli in the olfactory bulb. J Comp Neurol 524:199-
716 209.
717

718 Buck L, Axel R (1991) A novel multigene family may encode odorant receptors: a
719 molecular basis for odor recognition. Cell 65:175-187.
720

721 Chess A, Simo, I, Cedar H, Axel R (1994) Allelic inactivation regulates olfactory receptor
722 gene expression. Cell 78:823-834.
723

724 Dal Col JA, Matsuo T, Storm DR, Rodriguez I (2007) Adenylyl cyclase-dependent axonal
725 targeting in the olfactory system. Development 134:2481-2489.
726

727 Dibattista M, Reisert J (2016) The odorant receptor-dependent role of olfactory marker
728 protein in olfactory receptor neurons. J Neurosci 36:2995-3006.
729

730 Feinstein P, Mombaerts P (2004) A contextual model for axonal sorting into glomeruli in
731 the mouse olfactory system. Cell 117:817-831.
732
733 Feinstein P, Bozza T, Rodriguez I, Vassalli A, Mombaerts P (2004) Axon guidance of
734 mouse olfactory sensory neurons by odorant receptors and the β2 adrenergic receptor.
735 Cell 117:833-846.
736
737 Gu C, Rodriguez ER, Reimert DV, Shu T, Fritzsch B, Richards LJ, Kolodkin AL, Ginty
738 DD (2003) Neuropilin-1 conveys semaphorin and VEGF signaling during neural and
739 cardiovascular development. Dev Cell 5, 45-57.
740
741 Imai T, Suzuki M, Sakano H (2006) Odorant receptor-derived cAMP signals direct
742 axonal targeting. Science 314:657-661.
743
744 Imai T, Yamazaki T, Kobayakawa R, Kobayakawa K, Abe T, Suzuki M, Sakano H (2009)
745 Pre-target axon sorting establishes the neural map topography. Science 325:585-590.
746
747 Ishii T, Serizawa S, Kohda A, Nakatani H, Shiroishi T, Okumura K, Iwakura Y, Nagawa
748 F, Tsuboi A, Sakano H (2001) Monoallelic expression of the odourant receptor gene and
749 axonal projection of olfactory sensory neurones. Genes Cells 6:71-78.
750

751 Li J, Ishii T, Feinstein P, Mombaerts P (2004) Odorant receptor gene choice is reset by
752 nuclear transfer from mouse olfactory sensory neurons. Nature 428:393-399.
753
754 Liman ER, Corey DP, Dulac C (1999) TRP2: a candidate transduction channel for
755 mammalian pheromone sensory signaling. Proc Natl Acad Sci USA 96:5791-5796.
756
757 Luo, L (2015) Principles of Neurobiology, pp308-309. New York and London: Garland
758 Science.
759
760 Matsuo T, Aharony Rossier D, Kan C, Rodriguez I (2012) The wiring of Grueneberg
761 ganglion axons is dependent on neuropilin 1. Development 139: 2783-2791.
762
763 Mayer C, Acosta-Martinez M, Dubois SL, Wolfe A, Radovick S, Boehm U, Levine JE
764 (2010) Timing and completion of puberty in female mice depend on estrogen receptor a-
765 signaling in kisspeptin neurons. Proc Natl Acad USA Sci USA 52:22693-22698.
766
767 Mombaerts P (2006) Axonal wiring in the olfactory system. Annu Rev Cell Dev Biol
768 22:713-737.
769
770 Mombaerts P, Wang F, Dulac C, Chao SK, Nemes A, Mendelsohn M, Edmondson J, Axel
771 R (1996) Visualizing an olfactory sensory map. Cell 87:675-686.
772

773 Moriyoshi K, Richards LJ, Akazawa C, O'Leary DD, Nakanishi S (1996) Labeling neural
774 cells using adenoviral gene transfer of membrane-targeted GFP. Neuron 16:255-260.
775
776 Nagao H, Yoshihara Y, Mitsui S, Fujisawa H, Mori K (2000) Two mirror-image sensory
777 maps with domain organization in the mouse main olfactory bulb. NeuroReport 11,
778 3023-3027.
779
780 Nakashima A, Takeuchi H, Imai T, Saito H, Kiyonari H, Abe T, Chen M, Weinstein LS,
781 Yu CR, Storm DR, Nishizumi H, Sakano H (2013) Agonist-independent GPCR activity
782 regulates anterior-posterior targeting of olfactory sensory neurons. Cell 154:1314-1325.
783
784 Novak A, Guo C, Yang W, Nagy A, Lobe CG (2000) Z/EG, a double reporter mouse line
785 that expresses enhanced green fluorescent protein upon Cre-mediated excision. Genesis
786 28:147-155.
787
788 Omura M, Mombaerts P (2014) Trpc2-expressing sensory neurons in the main olfactory
789 epithelium of the mouse. Cell Rep 8:583-595.
790
791 Omura M, Mombaerts P (2015) Trpc2-expressing sensory neurons in the mouse main
792 olfactory epithelium of type B express the soluble guanylate cyclase Gucy1b2. Mol Cell
793 Neurosci 65:114-124.
794

795 Pasterkamp RJ, De Winter F, Holtmaat AJ, Verhaagen J (1998) Evidence for a role of the
796 chemorepellent semaphorin III and its receptor neuropilin-1 in the regeneration of
797 primary olfactory axons. J Neurosci 18:9962-9976.
798
799 Potter SM, Zheng C, Koos DS, Feinstein P, Fraser SE, Mombaerts P (2001) Structure and
800 emergence of specific olfactory glomeruli in the mouse. J Neurosci 21:9713-9723.
801
802 Ragan T, Kadiri LR, Venkataraju KU, Bahlmann K, Sutin J, Taranda J, Arganda-Carreras
803 I, Kim Y, Seung HS, Osten P (2012) Serial two-photon tomography for automated ex
804 vivo mouse brain imaging. Nat Methods 9:255-258.
805
806 Renier N, Wu Z, Simon DJ, Yang J, Ariel P, Tessier-Lavigne M (2014) iDISCO: a simple,
807 rapid method to immunolabel large tissue samples for volume imaging. Cell 159:896-
808 910.
809
810 Richard MB, Taylor SR, Greer CA (2010) Age-induced disruption of selective olfactory
811 bulb synaptic circuits. Proc Natl Acad Sci USA 107:15613-15618.
812
813 Saraiva LR, Ibarra-Soria X, Khan M, Omura M, Scialdone A, Mombaerts P, Marioni JC,
814 Logan DW (2015) Hierarchical deconstruction of mouse olfactory sensory neurons: from
815 whole mucosa to single-cell RNA-seq. Sci Rep 5:18178.
816

817 Schwarting GA, Kostek C, Ahmad N, Dibble C, Pays L, Püschel A (2000) Semaphorin 3A
818 is required for guidance of olfactory axons in mice. J Neurosci 20:7691-7697.
819
820 Schwarting GA, Raitcheva D, Crandall JE, Burkhardt C, Püschel A (2004) Semaphorin
821 3A-mediated axon guidance regulates convergence and targeting of P2 odorant receptor
822 axons. Eur J Neurosci 19:1800-1810.
823
824 Strotmann J, Conzelmann S, Beck A, Feinstein P, Breer H, Mombaerts P (2000) Local
825 permutations in the glomerular array of the mouse olfactory bulb. J Neurosci 20:6927-
826 6938.
827
828 Taniguchi M, Nagao H, Takahashi YK, Yamaguchi M, Mitsui S, Yagi T, Mori K, Shimizu
829 T (2003) Distorted odor maps in the olfactory bulb of semaphorin 3A-deficient mice. J
830 Neurosci 23:1390-1397.
831
832 Vassalli A, Rothman A, Feinstein P, Zapotocky M, Mombaerts P (2002) Minigenes
833 impart odorant receptor-specific axon guidance in the olfactory bulb. Neuron 35:681-
834 696.
835
836 Vassalli A, Feinstein P, Mombaerts P (2011) Homeodomain binding motifs modulate the
837 probability of odorant receptor gene choice in transgenic mice. Mol Cell Neurosci
838 46:381-396.

Wen S, Götze IN, Mai O, Schauer C, Leinders-Zufall T, Boehm (2011) New model for studying neural circuits underlying reproductive physiology in the mouse brain. Endocrinology 152, 1515-1526.

Zapiec B, Mombaerts P (2015) Multiplex assessment of the positions of odorant receptor-specific glomeruli in the mouse olfactory bulb by serial two-photon tomography. Proc Natl Acad Sci USA 112:E5873-5882.

Zou DJ, Feinstein P, Rivers AL, Mathews GA, Kim A, Greer CA, Mombaerts P, Firestein S (2004) Postnatal refinement of peripheral olfactory projections. Science 304, 1976-1979.

Zou DJ, Chesler AT, Le Pichon CE, Kuznetsov A, Pei X, Hwang EL, Firestein S (2007) Absence of adenylyl cyclase 3 perturbs peripheral olfactory projections in mice. J Neurosci 27:6675-6683.

855 **Legends**

856 **Figure 1.**
857
858 **Epifluorescence wholemount images of bulbs of gene-targeted mice expressing M71**
859 **and GFP with and without Nrp1.**

860

861 Images of dorsal views of both bulbs were taken with a Nikon SMZ25 stereomicroscope.
862 Signals represent the intrinsic fluorescence of GFP. Anterior is up, posterior is down, left
863 is left, and right is right.

864

865 ***A***, mouse homozygous for M71-IRES-tauGFP at PD21.

866

867 ***B***, mouse homozygous for M71-IRES-Cre and homozygous for the R26-tauGFP41 Cre
868 reporter at PD21.

869

870 ***C***, triple-mutant n5247MCZ mouse at PD14.

871

872 ***D***, triple-mutant n5247MCZ mouse at PD21.

873

874 Medial and lateral M71 glomeruli at the endogenous positions are indicated with green
875 and yellow arrows, respectively. Ectopic glomeruli in the conditional *Nrp1* knockout are
876 indicated with pink arrows (ectopic anterior) and blue arrows (ectopic dorsal). Scale
877 bars, 100 μm.

878

879 **Figure 2.**
880
881 **Configurations of M71 glomeruli in bulbs of conditional *Nrp1* knockout mice.**

882

883 ***A***, triple-mutant mice n5247MCZ, and ***B***, quadruple-mutant mice NMRCZ. The
884 occurrence of configurations I-VI is listed per age. Red numbers indicate the most
885 frequent configuration for a given age. Positions of labeled glomeruli in the various
886 configurations are illustrated schematically with green dots, and in the case of NMRCZ
887 with orange dots for glomeruli that consist clearly of both RFP+ and GFP+ axons, and
888 green dots for glomeruli formed predominantely by GFP+ axons. No glomeruli formed
889 by only RFP+ axons were observed. The data are pooled from whole-mount images and
890 coronal sections. Pairwise Chi-squared tests with Bonferroni correction for multiple
891 comparisons were performed on successive age pairs for both strains: n5247MCZ: PD0
892 vs PD14 (*), PD14 vs PD21 (n.s.), PD21 vs PD105 (***); NMCZ: PD7 vs PD14 (n.s.), PD14
893 vs PD21 (n.s.), PD21 vs PD35 (n.s.), PD35 vs PD45 (n.s.), PD45 vs PD 70 (*). The pre
894 multiple-comparison sigma values are designated as * $p<0.05$, ** $p<0.01$, *** $p<0.001$.
895

896 **Figure 3.**

897 **Three-dimensional reconstructions of bulbs of PD21 gene-targeted mice expressing**

898 **M71 with and without Nrp1.**

899

900 Serial block-face two-photon tomography was carried out to image the intrinsic

901 fluorescence in four bulbs of four homozygous M71-IRES-tauYFP mice at PD21, and in

902 six bulbs of six triple-mutant n5247MCZ mice at PD21. Each individual mouse is

903 indicated with a distinct color. The gray outer area represents the surface of the

904 glomerular layer, and the black inner area the regions of the bulb below the glomerular

905 layer. ***A***, dorsal view, comparable to the view in Figure 1. The medial M71 glomeruli are

906 poorly visible in this dorsal view, because they reside in a flat, medial domain of the

907 bulb. ***B***, dorsomedial view. The ectopic anterior glomeruli reside in the rostral tip of the

908 bulb. Both the medial and lateral glomeruli are visible here by making the glomerular

909 layer transparent. The bulb is tilted slightly laterally to expose the medial glomeruli

910 better. **C**, close-ups of views oriented in such a way that the individual glomeruli are

911 separated clearly: dorsal, anterior, and medial domains of the bulb.

912

913

914 **Figure 4.**

915 **Confocal and wholemount imaging of M71 glomeruli in triple-mutant NMCZ and**

916 **quadruple-mutant NMRCZ mice.**

917

918 ***A***, ***B***, horizontal 12 µm sections of bulbs of NMCZ mice at PD21 imaged with a Zeiss

919 LSM 710 confocal microscope, using the intrinsic fluorescence of GFP and

920 counterstaining of nuclei with DAPI. The box indicated with a white stippled line in the

921 left images is magnified in the right images. ***A***, ectopic dorsal glomerulus, large. ***B***,

922 ectopic anterior glomerulus, small and located deeper in the glomerular layer. ***C-H***,

923 wholemount bulbs of an NMRCZ mouse at PD59 imaged in widefield on a Nikon

924 SMZ25 stereofluorescence microscope. ***C***, dorsal view of the left and right bulbs, with

925 the left bulb exhibiting configuration VI, and the right bulb configuration V. Not all

926 glomeruli are visible in this view. ***D***, the right bulb from ***C*** (white box) is tilted to the

927 right in order to provide a better view of the medial aspect and demonstrate the

928 configuration consisting of an ectopic anterior glomerulus (blue box), a medial

929 glomerulus (red box), and an ectopic dorsal glomerulus (orange box). ***E***, magnified view

930 of the ectopic anterior glomerulus and consisting of GFP+ axons, as shown in the blue

931 box in ***D***. ***F***, magnified view of the two dorsal glomeruli of the left bulb, in the yellow

932 box in ***C***. The left glomerulus exhibits a mixed, comparable contribution of GFP+ and

933 RFP+ axons. The right glomerulus consists mostly of GFP+ axons, with a compartment

934 of RFP+ axons. ***G***, magnified view of the mixed GFP+ RFP+ medial glomerulus of the

935 right bulb, as shown in the red box in ***D***. ***H***, magnified view of the ectopic dorsal

936 glomerulus consisting predominantly of GFP+ axons, as shown in the orange box in ***D***.
937 A small compartment of this glomerulus is innervated by an axon bundle containing
938 also RFP+ axons (pink arrow). ***I, J,*** 12 µm sections of bulbs of NMRCZ mice at PD56 and
939 PD70, respectively, imaged with a Zeiss LSM 710 confocal microscope, using the
940 intrinsic fluorescence of GFP and RFP and counterstaining of nuclei with DAPI. ***I***,
941 ectopic dorsal glomerulus consisting of RFP+ and GFP+ axons. ***J***, magnified view of an
942 ectopic-anterior glomerulus consisting of GFP+ axons.
943
944 Scale bars, ***A*** left, 100 µm; ***A*** right, 50 µm; ***B*** left, 100 µm; ***B*** right, 50 µm; ***C, D***, 300 µm; **E**,
945 20 µm; ***F***, 50 µm; ***G***, 25 µm; ***H***, 50 µm; ***I, J,*** 25 µm.
946
947

948 **Figure 5.**

949 **Numbers of labeled cells per mouse in mice with gene-targeted mutations in the *M71***

950 **locus at PD21.**

951

952 Number are given ±SD and are Abercrombie-corrected, as described in Bressel et al.,

953 2016. A symbol represents an individual mouse. The numbers for M71-IRES-tauGFP

954 (n=5 mice) and M71-IRES-tauRFP2 (n=3 mice) are taken from Bressel et al., 2016 for

955 comparison. "M71-IRES-Cre heterozygous" and "M71-IRES-tauRFP2 heterozygous" are

956 the numbers of labeled cells representing the two different M71 alleles in NMRCZ (n=4

957 mice), and the sum of these numbers is given in "NMRCZ". The symbols (asterisk,

958 upward triangle, downward triangle, diamond) used for NMRCZ represent individual

959 mice. Analysis of cell counts using one-way ANOVA found all homozygous vs

960 heterozygous pairs significant ($p<0.05$) according to Tukey's Multiple Comparison Test,

961 which is consistent with monoallelic expression of OR genes. All other comparisons (-/-

962 vs -/- pairs and +/- vs +/- pairs) are not significant.

Figure 6.

Posterior glomeruli in the vicinity of Gucy1b2+ glomeruli can be Nrp1+ or Nrp1-.

Fluorescence images of three horizontal sections of a bulb of a homozygous Gucy1b2-IRES-tauGFP mouse at 4 weeks were taken with a Zeiss LSM 710 confocal microscope. Each of the three Gucy1b2+ glomeruli is indicated with a yellow arrowhead.

A, Section at a very ventral level, 0.13 mm from the bottom of the bulb, as shown schematically in ***D***. Intrinsic GFP fluorescence (GFP*) is combined with immunofluorescence for Nrp1 (red) and Adcy3 (blue). Nuclear staining with DAPI is in white. Merged is all colors together. The top four panels show the entire section. The bottom four panels show high-magnification views of an area surrounding the GFP+ glomerulus. This glomerulus is Adcy3- and Nrp1-. The posterior part of the bulb at this very ventral level level is devoid of Nrp1 immunofluorescence but contains numerous glomeruli that are Adcy3+.

B, Section at a more dorsal level, 0.29 mm from the bottom of the bulb. The image on the left shows the entire section. The two panels on the right show high-magnification views of an area surrounding the GFP+ glomerulus. This extremely posterior GFP+ glomerulus is Adcy3- and Nrp1-. The glomerulus anterior to the GFP+ glomerulus is Adcy3+ and Nrp1+ (yellow arrow), but the glomerulus posterior to the GFP+ glomerulus is Adcy3+ and Nrp1- (unfilled yellow arrowhead).

C, Section at an intermediate dorsal-ventral level, 1.24 mm from the bottom of the bulb. The image on the left shows the entire section. The two panels on the right show high-magnification views of an area surrounding the GFP+ glomerulus. This very posterior GFP+ glomerulus is Adcy3- and Nrp1-. The glomeruli anterior to it are strongly Adcy3+ and Nrp1-, and the most anterior glomerulus (indicated with an arrow) is Adcy3+ and weakly Nrp1+.

D, Schematic diagram of a medial view on the bulb. The positions of the three glomeruli shown in ***A-C*** are indicated.

Scale bars, ***A***, top 200 µm, bottom 50 µm; ***B***, ***C***, left 200 µm, right 50 µm.
a, anterior; p, posterior; m, medial; l, lateral; glom, glomerulus.

1001 **Figure 7.**

1002 **Three-dimensional reconstructions of bulbs with Nrp1 immunofluorescence levels in**

1003 **glomeruli of a bulb of a wild-type C57BL6/J mouse at PD14.**

1004

1005 After iDISCO treatment of the bulb, immunofluorescence with antibodies against Nrp1

1006 and VGLUT2 was applied to the wholemount, followed by serial block-face two-photon

1007 tomography and 3D reconstruction.

1008

1009 ***A***, Overall Nrp1 immunofluorescence signal, medial view on the bulb. The lookup table

1010 from low (blue) to high (green) represents the intensity of the overall Nrp1

1011 immunofluorescence signal, which is much stronger in axons than in glomeruli. The

1012 signal in glomeruli is mostly obscured by the signal in overlying axons.

1013

1014 ***B***, Segmented VGLUT2 immunofluorescence signal, shown in uniform green, binary

1015 signal, with no intensity information. VGLUT2 is a marker for OSN axon terminals

1016 within glomeruli. The layers of the bulb below the glomerular layer are rendered in

1017 black for contrast and orientation.

1018

1019 ***C***, Medial view of the reconstructed bulb. The Nrp1 signal is confined to glomeruli by

1020 generating a mask using the VGLUT2 signal. The lookup table from low (violet) to high

1021 (red) represents the intensity of the Nrp1 immunofluorescence signal in glomeruli.

Generally, anterior glomeruli are Nrp1-low (from violet to blue), and generally, posterior glomeruli are Nrp1-high (from green over yellow to red).

D, Lateral view of the reconstructed bulb. Generally, anterior glomeruli are Nrp1-low, and generally, posterior glomeruli are Nrp1-high.

1028 **Figure 8.**
1029
1030 **Epifluorescence wholemount images of bulbs of transgenic mice expressing rat OR I7**
1031 **from a mouse MOR23 promoter and gap-YFP with and without Nrp1.**
1032
1033 Images of medial views of bulbs were taken with a Nikon SMZ25 stereomicroscope.
1034 Signal represents the intrinsic fluorescence of gap-YFP. Dorsal is up, ventral is down.
1035
1036 ***A***, Views on the medial and lateral aspects of a left bulb (left two images) and a right
1037 bulb (right two images) of two I7-Cre-YFP Tg mice at PD17. Axons coalesce into a single
1038 glomerulus.
1039
1040 ***B***, Views on the medial and lateral aspects of the right bulbs of six I7-Cre-YFP Tg x
1041 n5247-flox littermates at PD14. Images are pairwise for an individual mouse. Glomeruli
1042 are indicated with yellow arrows. Axons coalesce into multiple glomeruli, in particular
1043 in the lateral aspect.
1044

1045 **Figure 9.**

1046 **Example of a three-dimensional reconstruction of a bulb of a PD14 transgenic mouse**

1047 **expressing rat OR I7 from a mouse MOR23 promoter and gap-YFP.**

1048

1049 The right bulb of a mouse was reconstructed in 3D after epifluorescence wholemount

1050 imaging with a Nikon SMZ25 stereomicroscope. The images of the medial and lateral

1051 aspects of this bulb are the same as in Figure 8, right bottom, and reproduced here to

1052 facilitate comparison with the 3D reconstruction. There are two labeled glomeruli in the

1053 medial aspect (compared to two in the epifluorescence wholemount image, yellow

1054 arrows), and five labeled glomeruli in the lateral aspect (compared to four in the

1055 epifluorescence wholemount image, yellow arrows).

1056

1057

1058 **Figure 10.**

1059 **Three-dimensional reconstructions of bulbs of transgenic mice expressing rat OR I7**

1060 **from a mouse MOR23 promoter and gap-YFP with and without Nrp1.**

1061

1062 For PD14, three bulbs of three I7-Cre-YFP Tg littermates (indicated in shades of gray)

1063 and eight bulbs of seven I7-Cre-YFP Tg x n5247-flox littermates (indicated in distinct

1064 colors) were reconstructed. For one mouse, both the left and right bulbs (green and

1065 turquoise) are included in the merged bulb. For PD21, three bulbs of three I7-Cre-YFP

1066 Tg x n5247-flox littermates were reconstructed. Views are medial, lateral, and ventral.

1067

1068 ***A***, merged bulb of three I7-Cre-YFP Tg bulbs at PD14.

1069

1070 ***B***, merged bulb of three I7-Cre-YFP Tg bulbs at PD14 together with eight I7-Cre-YFP Tg

1071 x n5247-flox bulbs at PD14. Because of the large number of glomeruli depicted, the gray-

1072 transparent outer layer of the bulb shown in Figures 3 and 9 is here omitted. Medially,

1073 I7-Cre-YFP Tg x n5247-flox glomeruli are shifted anteriorly and ventrally, and scattered

1074 over a sector that is anchored on the tightly clustered I7-Cre-YFP Tg glomeruli.

1075 Laterally, I7-Cre-YFP Tg x n5247-flox glomeruli are shifted dorsally and ventrally, and

1076 scattered over a belt that is centered on the tightly clustered I7-Cre-YFP Tg glomeruli.

1077 This belt surrounds the anterior bulb as a U-shape, but is not continuous ventrally, as

1078 can be seen in the ventral view.

1079

1080 ***C***, merged bulb of three I7-Cre-YFP Tg x n5247-flox bulbs at PD21. These mice also
1081 contain the reporter ROSA-STOP-lacZ, but the taulacZ marker is not visualized. The
1082 number and degree of scattering of glomeruli is more pronounced than at PD14.
1083 **Movie 1**
1084 **3D animation of a merged bulb containing glomeruli from three M71-IRES-tauYFP**
1085 **bulbs and six n5247MCZ bulbs at PD21**
1086
1087 The merged bulb 3D reconstruction displays the positions of labeled glomeruli from a
1088 total of nine bulbs together, enabling a direct comparison of these positions. This
1089 animation provides multiple viewing angles of the merged bulb shown in Figure 3.
1090 Glomeruli from M71-IRES-tauYFP bulbs are rendered in cold colors (green/blue) as
1091 indicated by the legend in the top left, and glomeruli from n5247MCZ bulbs are in warm
1092 colors (pink/purple/red/orange/brown/yellow). The sequence starts with a view of
1093 the dorsal aspect of the bulb with the posterior-dorsal glomeruli from M71-IRES-tauYFP
1094 bulbs visible near the bottom, and the posterior-medial glomeruli visible in a small
1095 cluster near the left of the screen. As the camera pans to reveal the medial aspect of the
1096 bulb, the glomeruli from n5247MCZ bulbs are revealed sequentially. The camera then
1097 progresses along the medial aspect of the bulb from posterior to anterior, before
1098 panning out to stop on a long view of the medial aspect of the bulb.
1099

Movie 2

3D animation of a merged bulb containing glomeruli from three PD14 I7-Cre-YFP-Tg bulbs, eight PD14 I7-Cre-YFP-Tg x n5247 bulbs, and three PD21 I7-Cre-YFP-Tg x n5247 bulbs

The animation begins with a view of the medial aspect of the merged bulb with anterior located to the left and dorsal on top. Three glomeruli, each from a different PD14 I7-Cre-YFP Tg mouse, are displayed together with the shade of gray indicating the identity. The legends on the top left and bottom left of the screen indicate the strain of all glomeruli shown. As the animaton proceeds, glomeruli from PD14 I7-Cre-YFP-Tg x n5247 bulbs are added sequentially. These glomeruli occupy a sector of the bulb extending roughly from the medial domain of PD14 I7-Cre-YFP-Tg glomeruli toward and beyond their lateral domain by way of the ventral ridge of the bulb. The ventral view of the bulb shown at the 11-second mark provides a clear view of the belt of glomeruli straddling the ventral aspect of the bulb. Finally, the glomeruli from PD14 bulbs are removed, and glomeruli from three PD21 I7-Cre-YFP-Tg bulbs are shown; these glomeruli occupy a broad sector of both the medial and lateral aspects.

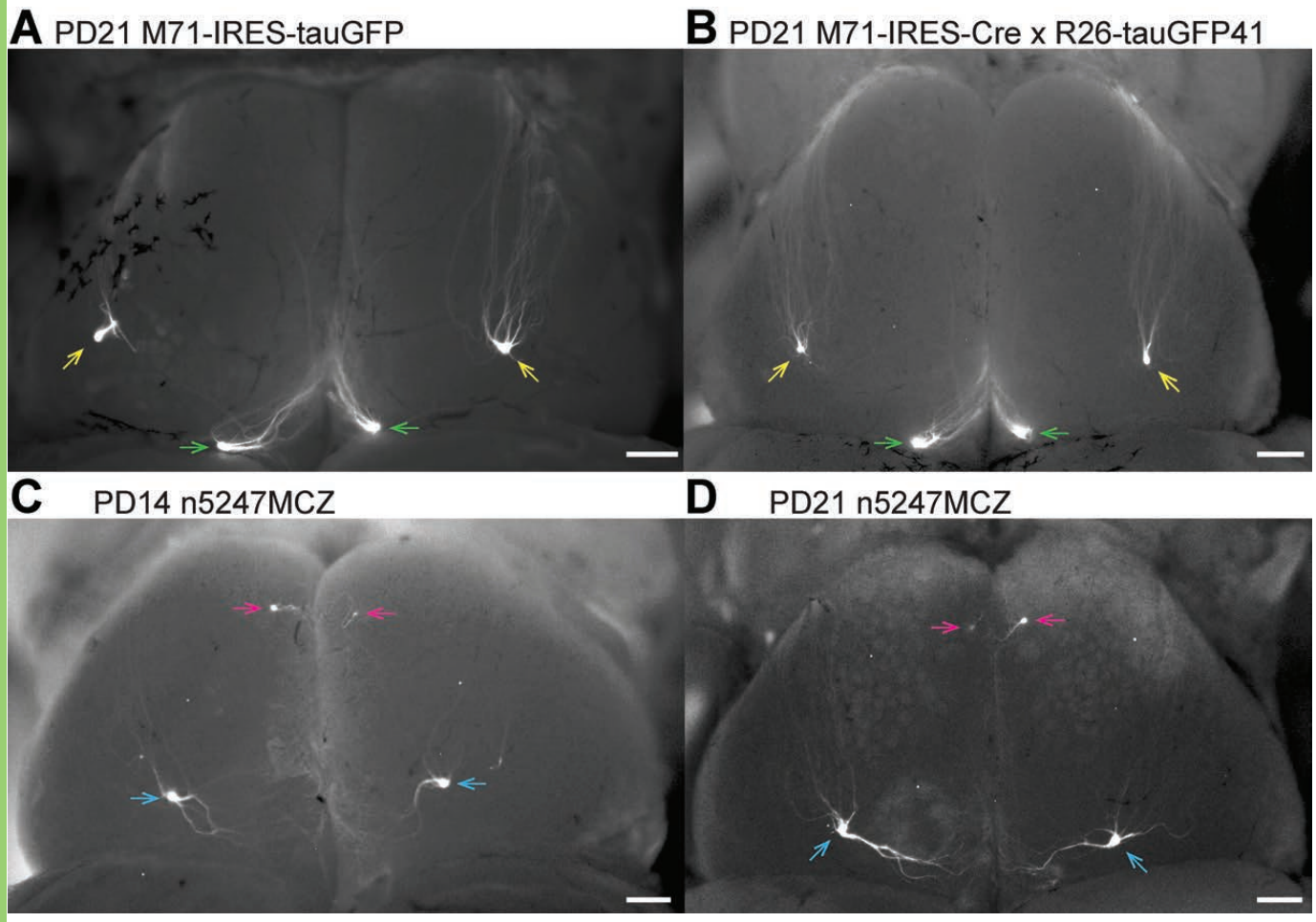

A

n5247MCZ

	Configuration	PD0 bulbs/total	PD14 bulbs/total	PD21 bulbs/total	PD45 bulbs/total	PD105 bulbs/total
I		7/10	2/8	11/21	2/2	0/4
II		1/10	6/8	9/21	0/2	0/4
III		2/10	0/8	0/21	0/2	2/4
IV		0/10	0/8	1/21	0/2	2/4

B

NMRCZ

	Configuration	PD7 bulbs/total	PD14 bulbs/total	PD21 bulbs/total	PD35 bulbs/total	PD45 bulbs/total	PD70 bulbs/total
I		1/3	2/8	1/13	0/11	0/4	0/4
III		0/3	0/8	0/13	0/11	2/4	0/4
IV		1/3	2/8	1/13	3/11	2/4	0/4
V		1/3	3/8	11/13	7/11	0/4	4/4
VI		0/3	1/8	0/13	1/11	0/4	0/4

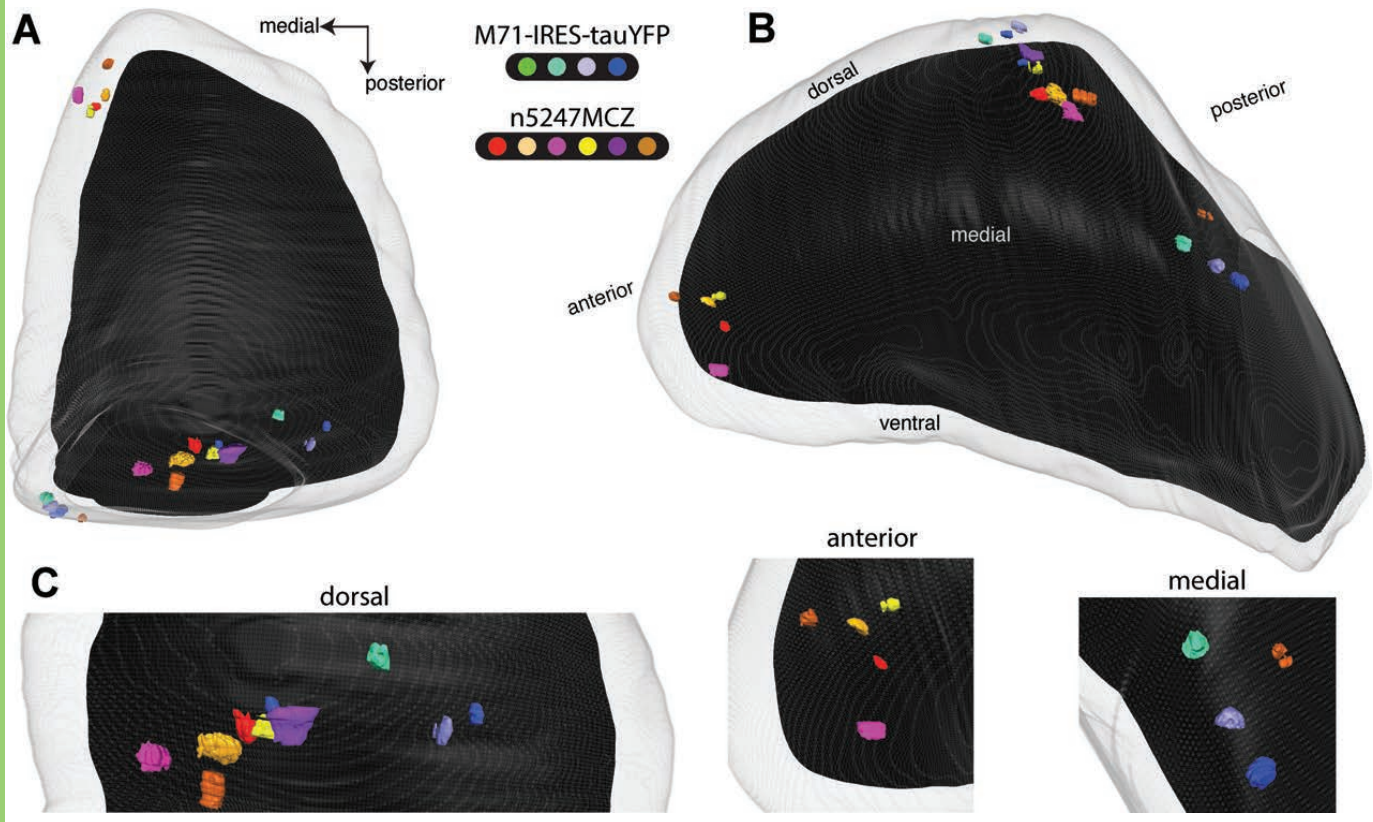

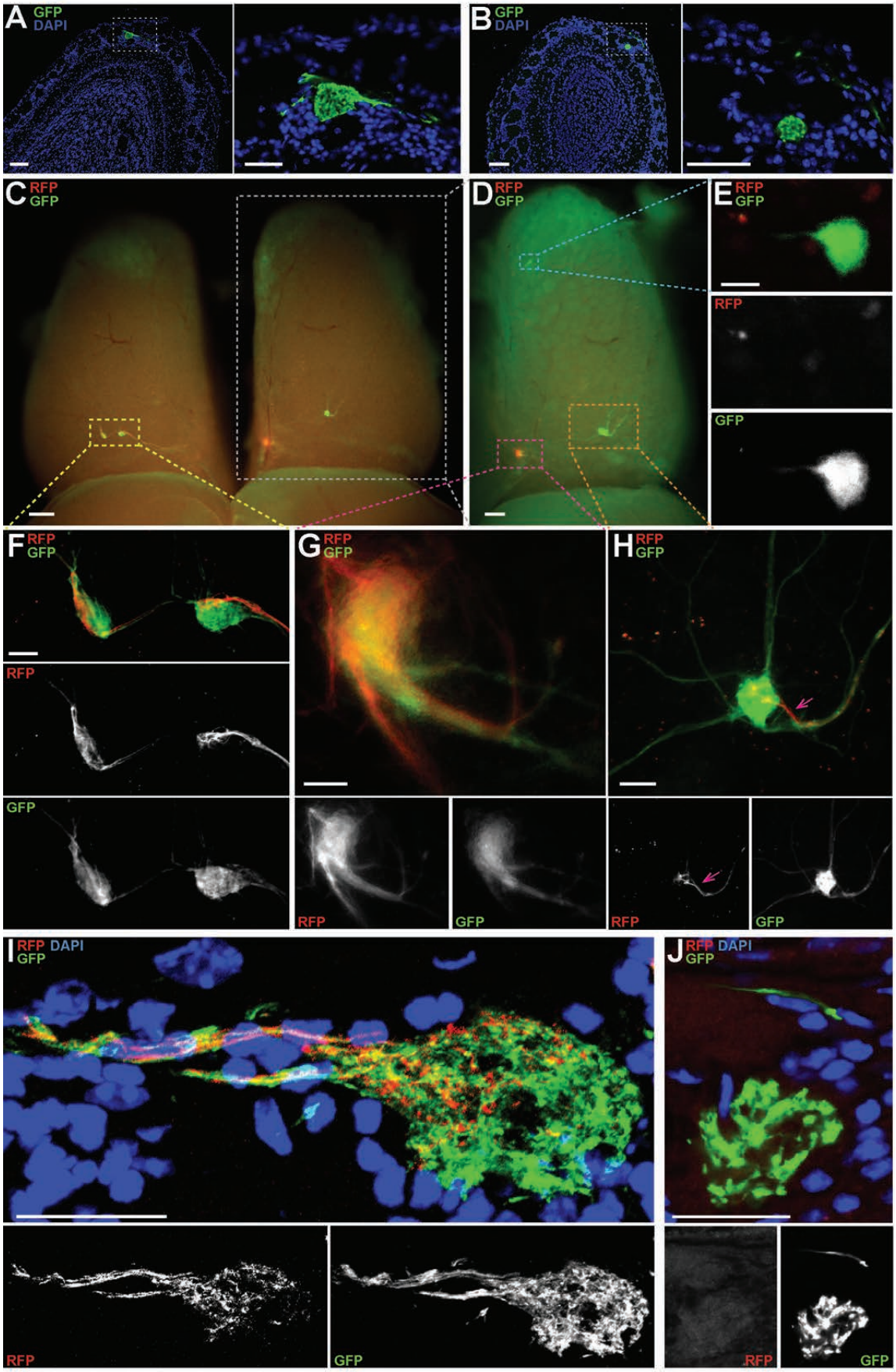

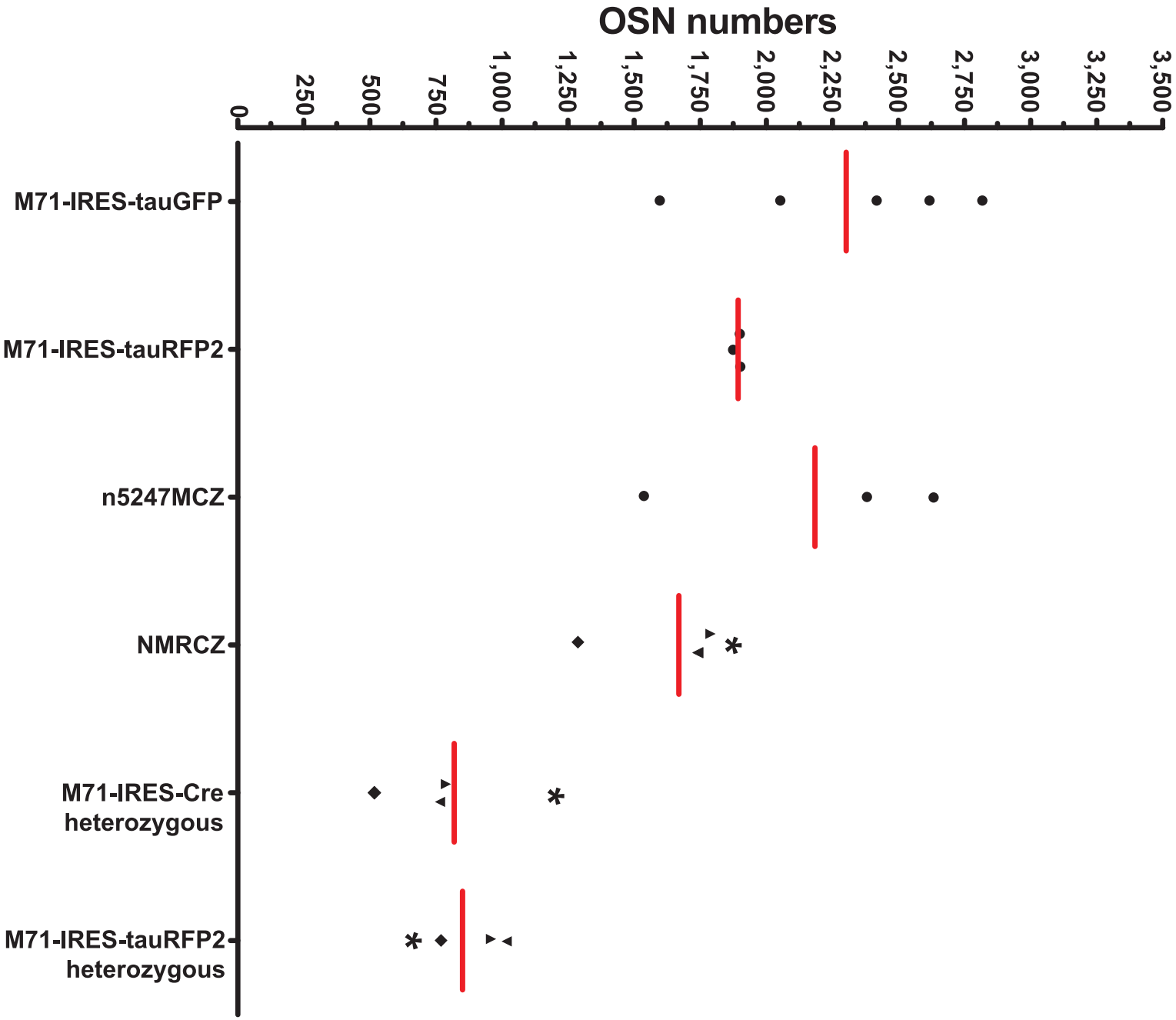
OSN numbers
0
250
500
750
1,000
1,250
1,500
1,750
2,000
2,250
2,500
2,750
3,000
3,250
3,500
M71-IRES-tauGFP
M71-IRES-tauRFP2
n5247MCZ
NMRCZ
M71-IRES-Cre heterozygous
M71-IRES-tauRFP2 heterozygous

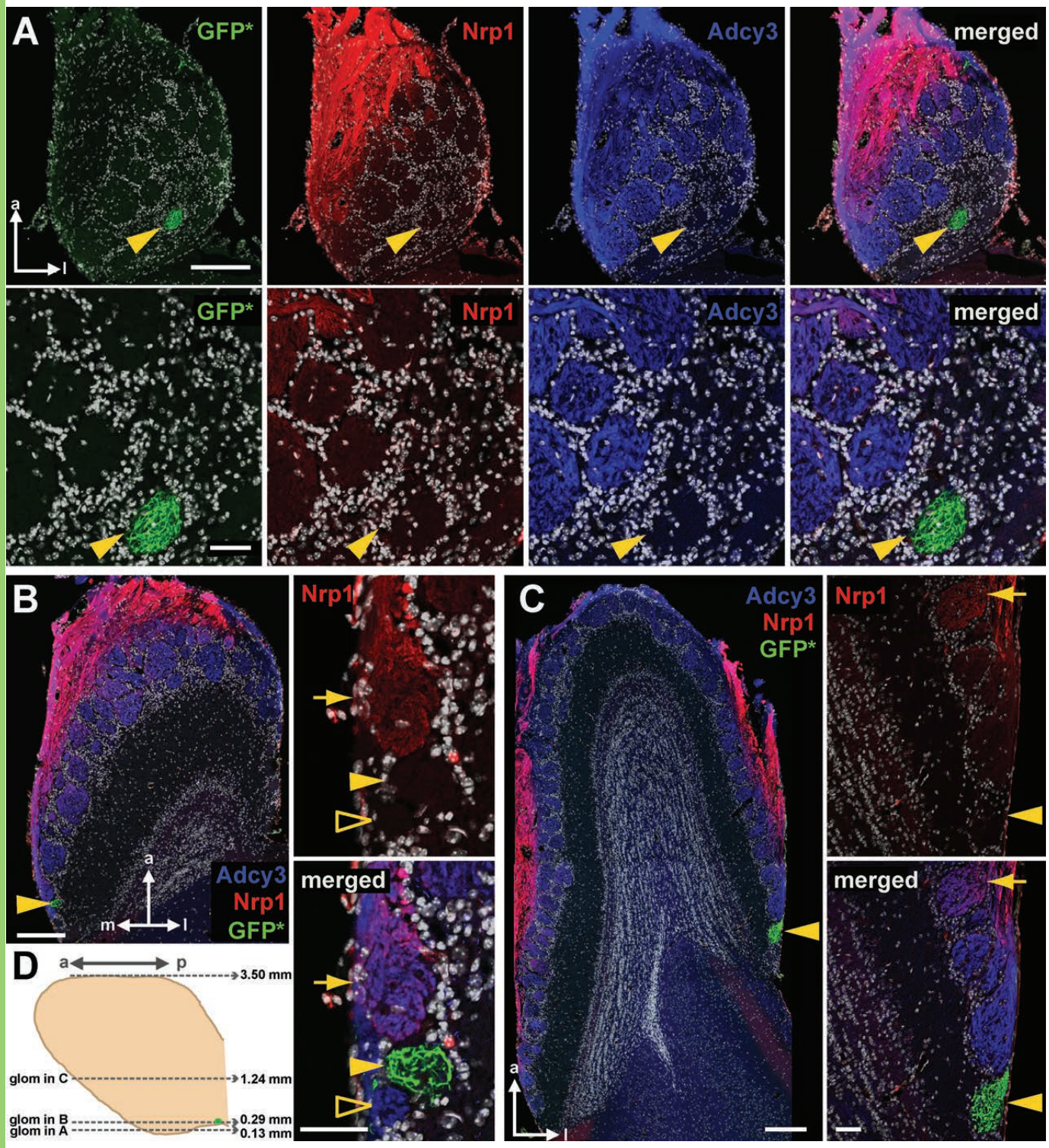

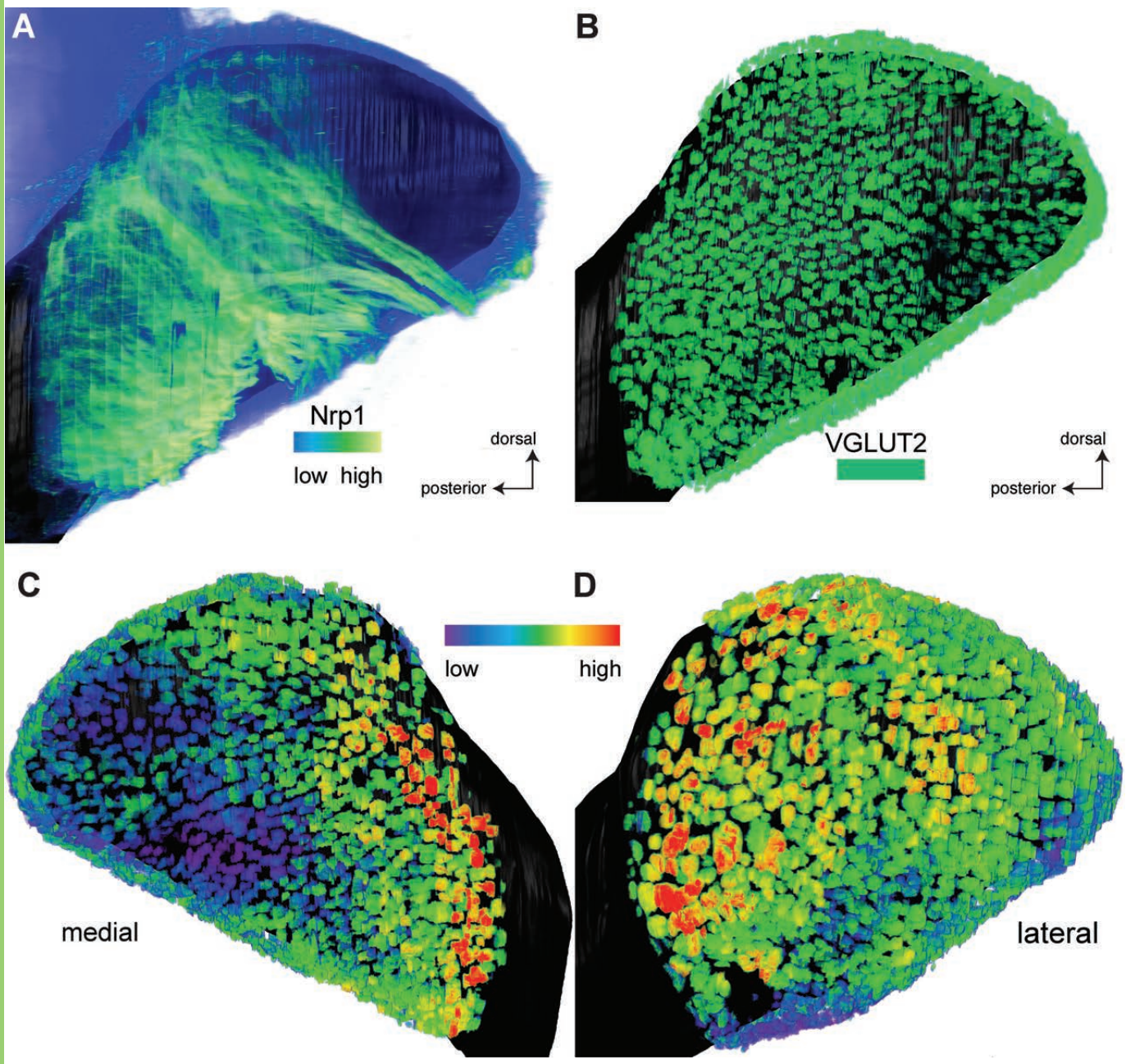

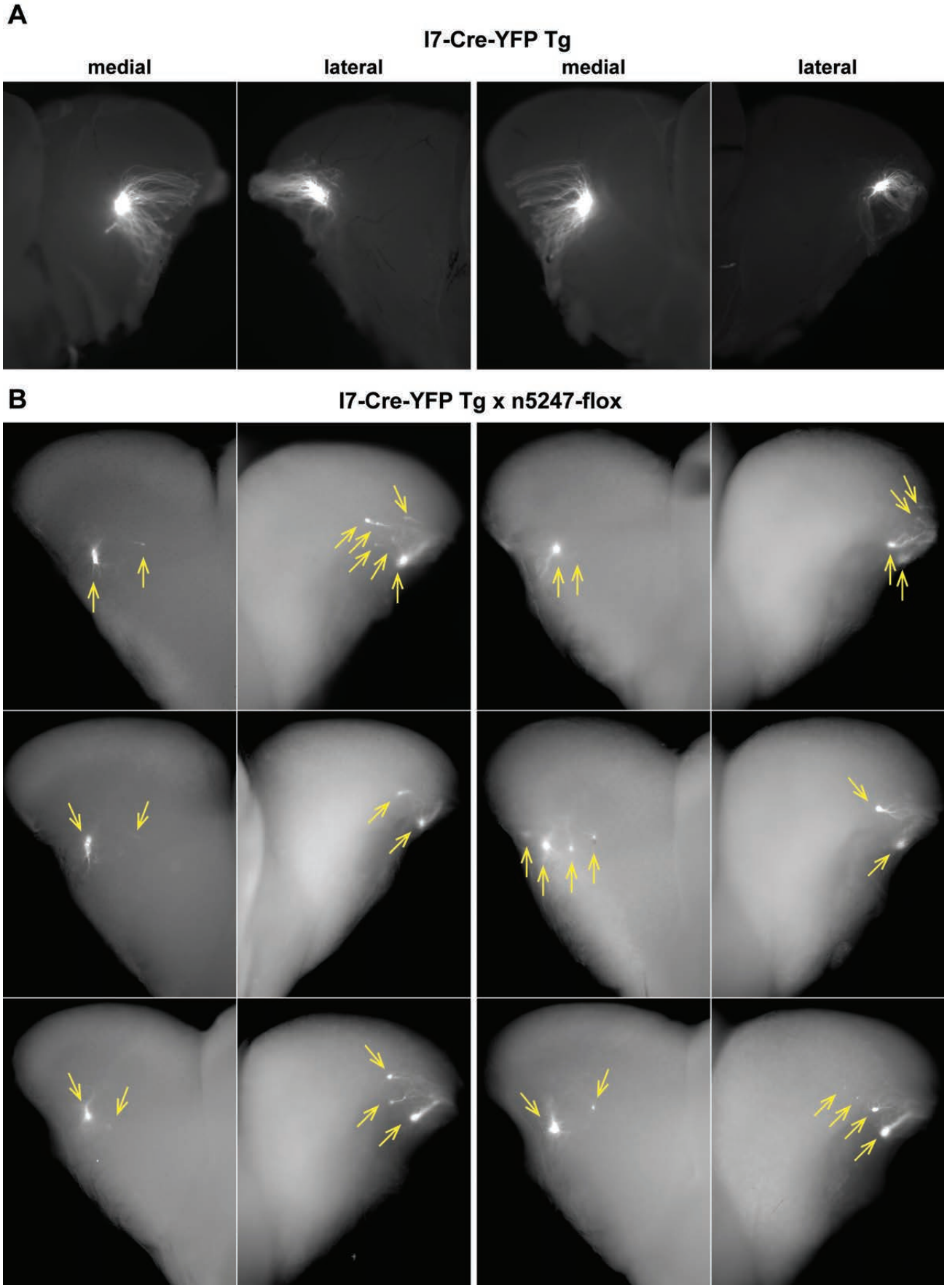

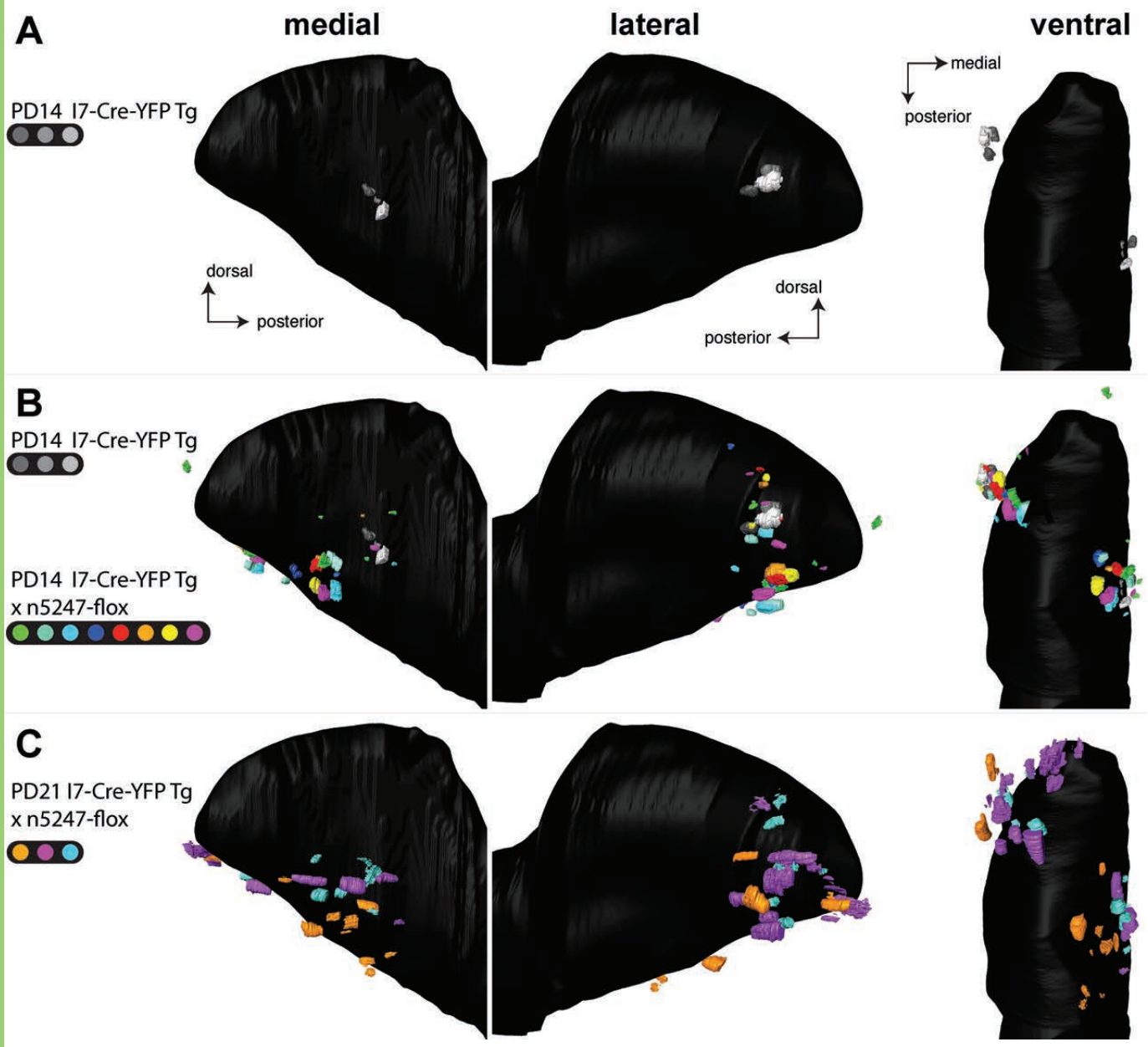

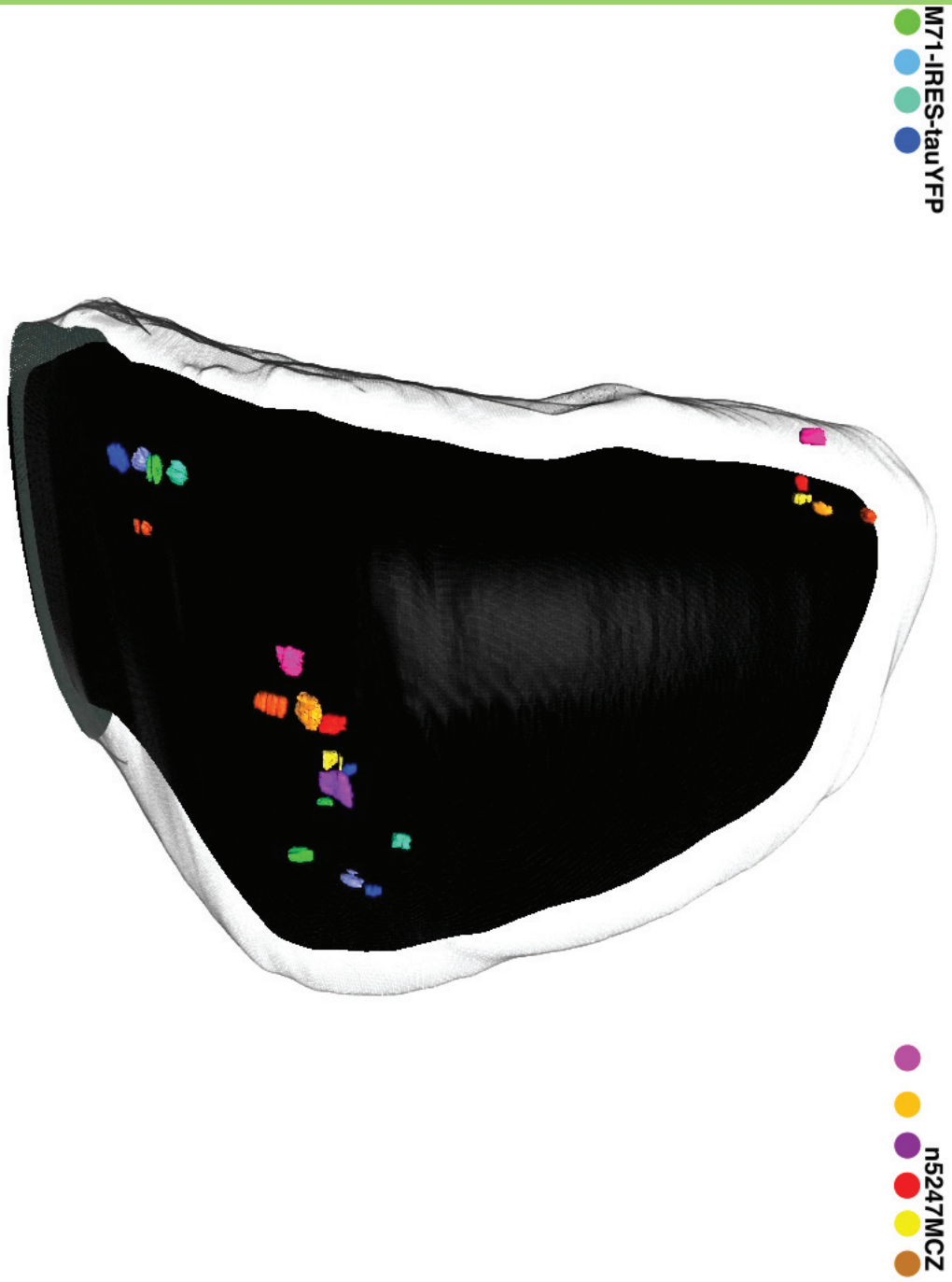
M71-IRES-tauYFP
n5247MCZ